ISTANBUL TECHNICAL UNIVERSITY ★ GRADUATE SCHOOL OF SCIENCE ENGINEERING AND TECHNOLOGY

PERFORMANCE BEHAVIOR OF COMPRESSED LIQUID GEOTHERMAL RESERVOIRS UNDER A CONSTANT ENERGY PRODUCTION SCHEME

M.Sc. THESIS

Gunay TAHIROVA

Department of Petroleum and Natural Gas Engineering

Petroleum and Natural Gas Engineering Programme

DECEMBER, 2016

ISTANBUL TECHNICAL UNIVERSITY ★ GRADUATE SCHOOL OF SCIENCE ENGINEERING AND TECHNOLOGY

PERFORMANCE BEHAVIOR OF COMPRESSED LIQUID GEOTHERMAL RESERVOIRS UNDER A CONSTANT ENERGY PRODUCTION SCHEME

M.Sc. THESIS

Gunay TAHIROVA
(505141506)

Department of Petroleum and Natural Gas Engineering

Petroleum and Natural Gas Engineering Programme

Thesis Advisor: Assoc. Prof. Ömer İnanç Türeyen

DECEMBER, 2016

İSTANBUL TEKNİK ÜNİVERSİTESİ ★ FEN BİLİMLERİ ENSTİTÜSÜ

SABİT ENERJİ ÜRETİM SENARYOSU ALTINDA SIKIŞTIRILMIŞ SIVI JEOTERMAL REZERVUARLARIN PERFORMANS DAVRANIŞI

YÜKSEK LİSANS TEZİ

Gunay TAHIROVA
(505141506)

Petrol ve Doğal Gaz Mühendisliği Anabilim Dalı

Petrol ve Doğal Gaz Mühendisliği Programı

Tez Danışmanı: Yard. Prof. Ömer İnanç Türeyen

ARALIK, 2016

Gunay Tahirova, a **M.Sc.** student of ITU **Institute of Energy** student ID 505141506, successfully defended the **thesis** entitled "Performance behavior of compressed liquid geothermal reservoirs under a constant energy production scheme", which she prepared after fulfilling the requirements specified in the associated legislations, before the jury whose signatures are below.

Thesis Advisor :	**Assoc. Prof. Ömer İnanç TÜREYEN** Istanbul Technical University	.....
Jury Members:	**Prof. Dr. Abdurrahman SATMAN** Istanbul Technical University	**.....**
	Prof. Dr. Serhat AKIN Middle East Technical University	.....

Date of Submission : 02 December 2016
Date of Defense : 23 December 2016

To my beloved husband, Orkhan,

for his encouragement and moral support

and to our families,

FOREWORD

I owe my special thanks to my advisor Assoc. Prof. Ömer İnanç TÜREYEN for guiding and supporting me all the time throughout the thesis study.

I would like to thank my thesis committee members for all of their guidance, discussion, ideas, and feedback.

Finally I want to express my sincere gratitudes to all my instructors, who have instilled in me academic discipline and work ethics and the amazing teaching staff of the Department of Petroleum and Natural Gas Engineering, at Istanbul Technical University.

December 2016 Gunay Tahirova

TABLE OF CONTENTS

Page

SYMBOLS

C **:** specific heat capacity
c : compressibility
e : energy
h **:** enthalpy
k **:** permeability
p **:** volumetric average pressure
T **:** temperature
t **:** time
u **:** internal energy
V **:** reservoir bulk volume
w **:** production rate

Greek Symbols

α **:** recharge constant
η **:** conversion efficiency
κ **:** reservoir storage capacity
ρ **:** density
ϕ **:** reservoir porosity

Subscripts

0 **:** initial conditions
i **:** injection
p **:** production
r **:** recharge source
ro **:** rock
ss **:** steady-state pressure
t **:** total reservoir (fluid and formation)
th **:** thermal
w **:** water

LIST OF TABLES

Page

LIST OF FIGURES

Page

PERFORMANCE BEHAVIOR OF COMPRESSED LIQUID GEOTHERMAL RESERVOIRS UNDER A CONSTANT ENERGY PRODUCTION SCHEME

SUMMARY

A reservoir model is a utility describing the change in reservoir pressure and temperature as a function of time or cumulative fluid production. Pressure and temperature are the main parameters to consider when modelling the geothermal reservoirs. Primary objectives of geothermal reservoir modeling are to estimate production capacity of the geothermal fields, the rate of reservoir pressure decline and the effects of fluid recharge and injection on field performance. There are mainly three methods of modeling available in the literature, which are decline curve analysis, numerical modeling and lumped parameter modeling.

Lumped parameter modeling, also known as zero-dimensional modeling, is a commonly used method when there is less data available at the early life of the field. In this model, reservoirs and aquifers are defined as homogeneous tanks and their average properties are used. Pressure and temperature behaviors are obtained by solving mass and energy conservation equations.

In the literature, many lumped parameter (tank) models have been proposed for isothermal and non-isothermal geothermal fields. However, most of these models are valid for constant flow rate production scenario.

In this study, a new non-isothermal single tank model was developed. Pressure and temperature behaviors are obtained by solving mass and energy conservation equations. With the new model developed, the temperature and pressure behaviors of the reservoir can be predicted for both scenarios, namely constant flow rate production and constant energy production scenarios.

The tank system used in the model to represent the geothermal system is a reservoir tank and a recharge source. In the model, the tank is assumed to be recharged from a constant pressure source from the outer edge of the tank. Natural recharge is considered by applying the Schilthuis steady state water influx model between the recharge source and the reservoir.

The main objective of this study is to compare reservoir performances under constant-energy and constant-flow production scenarios and to discuss the effects of certain parameters on reservoir performance behavior under constant energy production scenario.

From this study, it is concluded that for the assumed reservoir parameters, pressure and temperature at late time for constant energy production scenario stabilize at some value like in the constant flow rate production scenario. When flow rate production is considered under constant energy production scheme, it is observed that mass flow rate is dependent on temperature and and specific heat capacity of the water. While bulk volume affects pressure and temperature at early and middle times, it has no effect on the steady state pressure and temperature under both scenarios. Under constant energy production scheme, required energy value is observed to affect reservoir steady state pressure, however, it has no effect on the steady state temperature for constant energy production scheme. It is also observed that steady state pressure and temperature are not affected by the rock porosity. Since pressure and temperature at late time depend on the injection rate, they will stabilize at different values for each case of reinjection ratio. While recharge constant has no effect on the steady state temperature, it affects steady state pressure under constant energy production scheme.

SABİT ENERJİ ÜRETİM SENARYOSU ALTINDA SIKIŞTIRILMIŞ SIVI JEOTERMAL REZERVUARLARIN PERFORMANS DAVRANIŞI

ÖZET

Modelleme rezervuar basıncının ve sıcaklığının zamanla nasıl değiştiğini izlemek ve rezervuarın gelecek performansını değerlendirmek için kullanılan bir yöntemdir. Rezervuar modellemenin en yaygın üç yöntemi vardır. Sıfır boyutlu modelleme olarak da bilinen tank modelleri yöntemi yeni bulunan jeotermal sahalar için elde yeterli veri bulunmaması nedeniyle sıkça kullanılan bir yöntemdir. Bu modellemede rezervuarlar ve akifer ayrı birer homojen tank olarak tanımlanır ve ortalama özellikleri kullanılır. Kütle ve enerji korunum denklemlerinin çözülmesiyle basınç ve sıcaklık davranışları elde edilir.

Şimdiyedek literatürde izotermal ve izotermal olmayan jeotermal sahalar için birçok tank modelleri önerilmiştir. Ancak bu modellerin büyük kısmı sabit debili üretim için uygundur.

Bu çalışmada izotermal olmayan tek tank modeli geliştirilmiştir. Kütle ve enerji korunum denklemlerinin çözülmesiyle basınç ve sıcaklık davranışları elde edilmiştir. Geliştirilmiş yeni modelle hem sabit debili üretim, hem de sabit enerjili üretim senaryoları için rezervuarda oluşan sıcaklık ve basınç davranışları tahmin edilebilmektedir.

Modelde kullanılan tank sistemi bir rezervuar tankı ve beslenme kaynağı şeklindedir. Modelde rezervuar tankının dış sınırından sabit basınçlı bir beslenme kaynağından beslenmesi kabul edilmiştir. Beslenme kaynağı ve rezervuar arasındaki doğal beslenme için Schilthuis kararlı akış su girişi modeli kullanılmıştır.

Çalışmanın temel amacı sabit enerjili ve sabit debili üretim senaryoları altında rezervuar performanslarının kıyaslanması ve bazı parametrelerın sabit enerjili üretim zamanı rezervuar performansı üzerindeki etkilerinin tartışılmasıdır.

Çalışmada tek tank modelinde sabit enerjili ve sabit debili üretim senaryoları altında rezervuarın basınç ve sıcaklık davranışını incelemek için önce temel durum oluşturulmuş, daha sonra ise beş hipotetik durum önerilmiş ve analiz edilmiştir. Her durumda, tüm rezervuar parametreleri temel durumdakiyle aynı tutulmuş ve rezervuar performans davranışı üzerindeki etkisini görmek için yalnızca bir parametre değiştirilmiştir. Değişen parametreler kaba hacim, kurulu güç kapasitesi, gözeneklilik, tekrar basma oranı ve doğal beslenme endeksidir. Tüm durumlar sabit debili ve sabit enerjili üretim senaryoları altında incelenmiştir.

Temel durum için sabit debili ve sabit enerjili üretimde rezervuarın basınç ve sıcaklığının kararlı akışa ulaştığı görülmüştür. Rezervuar basıncının her iki senaryo için farklı değerlerde kararlı akışa ulaştığı görülse de, rezervuar sıcaklığının her iki senaryoda da aynı değerde kararlı akışa ulaştığı gözlemlenmiştir. Aynı zamanda üretimle birlikte rezervuar sıcaklığının azalması sebebiyle sabit enerji üretimi için akış

debisinin de zamanla arttığı ve geç zamanda sıcaklığın sabitlenmesiyle akış debisinin de sabitlendiği gözlemlenmiştir. Sabit enerjili üretim senaryosunun basınç davranışı incelendiğinde sabit debili üretimdeki basınç davranışından farklı olarak erken zamanda da sabitlendiği görülmüştür. Bunun sebebi rezervuar sıcaklığının erken zamanda çok az değişmesine karşılık akış debisinin ve dolayısıyla da basıncın stabil davranış sergilemesidir.

Birinci durumda kaba hacmin sabit debili ve sabit enerjili üretim senaryoları altında rezervuar basınç ve sıcaklık davranışları üzerindeki etkisi incelenmiştir. Rezervuar sıcaklığı her iki senaryoda da kaba hacimden bağımsız olarak aynı değerde kararlı akışa ulaşmıştır. Kaba hacim büyüdükçe sıcaklık ve basıncın daha geç kararlı akışa ulaştığı görülmüştür.

İkinci durumda kurulu güç kapasitesinin sabit debili ve sabit enerjili üretimde rezervuar performans davranışı üzerindeki etkisi incelenmiştir. Beklendiği gibi kurulu güç kapasitesi büyüdükçe rezervuar sıcaklığının daha erken kararlı akışa ulaştığı gözlemlenmiştir. Aynı zamanda geç zamanda basınç değerinin kurulu güç kapasitesine bağlı olduğu görülmüştür.

Üçüncü durumda gözenekliliğin her iki senaryo altında rezervuar basınç ve sıcaklık davranışları üzerindeki etkisi analiz edilmiştir. Gözenekliliğin erken zamanda sıcaklık ve basınç üzerindeki etkisi olsa da, geç zamanda basınç ve sıcaklığın gözeneklilikten bağımsız olduğu görülmüştür. Temel durumda olduğu gibi sabit enerjili üretim senaryosunun basınç davranışı incelendiğinde sabit debili üretimdeki basınç davranışından farklı olarak erken zamanda da sabitlendiği görülmüştür. Bunun sebebi yine rezervuar sıcaklığının erken zamanda çok az değişmesine karşılık akış debisinin ve dolayısıyla da basıncın stabil davranış sergilemesidir.

Dördüncü durumda tekrar basma oranının sabit debili ve sabit enerjili üretimde rezervuar performans davranışı üzerindeki etkisi incelenmiştir. Tekrar basma oranı büyüdükçe rezervuar sıcaklığının kararlı akış değerinin küçüldüğü gözlemlenmiştir. Rezervuar sıcaklığının kararlı akış değerinin beslenme kaynağı sıcaklığı ve tekrar basma sıcaklığıyla belirlendiği görülmüştür. Bu çalışmada beslenme kaynağı sıcaklığı ilkin rezervuar sıcaklığıyla aynı olduğundan ve tekrar basma sıcaklığı ilkin rezervuar sıcaklığından düşük olduğundan dolayı ne kadar az tekrar basma gerçekleştirilirse rezervuar sıcaklığının kararlı akış değerinin o kadar yüksek olduğu görülecektir. Sabit enerjili üretim senaryosunun basınç davranışı incelendiğinde tekrar basma oranının sıfır olduğu durumda basınç davranışının diğer durumlardan farklı olarak sabit debili üretimle aynı performansı gösterdiği görilmüştür. Bunun sebebi yine rezervuar sıcaklığının beslenme sıcaklığı ve tekrar basma sıcaklığıyla belirlenmiş olmasıdır. Tekrar basma gerçekleştirilmediği zaman rezervuar sıcaklığı aynı sıcaklıktakı beslenme kaynağından beslendiği için rezervuar sıcaklığında bir düşüş olmayacaktır. Dolayısıyla akış debisi sabit kalacak ve rezervuar basıncı sabit debili üretimle aynı performansı gösterecektir.

Beşinci durumda doğal beslenme endeksinin sabit debili ve sabit enerjili üretimde rezervuar performans davranışı üzerindeki etkisi incelenmiştir. Rezervuar sıcaklığı geç zamanda her iki senaryoda da doğal beslenme endeksinden etkilenmemiş olsa da, rezervuar basıncının doğal beslenme endeksine bağlı olduğu görülmüştür.

Sonuç olarak, bu çalışmada varsayılan rezervuar parametreleri için sabit debili üretimde olduğu gibi sabit enerjili üretimde de rezervuar basınç ve sıcaklığının geç zamanlarda belli bir değerde sabitlendiği gözlemlenmiştir. Sabit enerjili üretim zamanı debinin sıcaklık ve özgül ısı kapasitesine bağlı olduğu görülmektedir. Kaba hacim erken zamanlarda rezervuar basınç ve sıcaklığını etkilese de geç zamanlarda basınç ve sıcaklık üzerinde hiçbir ekisi yoktur.

Sabit enerjili üretimde kurulu güç kapasitesinin geç zamanlarda basınç üzerinde etkisinin olduğu, ama sıcaklık üzerinde etkisinin bulunmadığı gözlemlenmiştir. Rezervuar gözenekliliğinin geç zamanlarda basınç ve sıcaklık üzerinde hiçbir etkisi yoktur. Aynı zamanda basınç ve sıcaklık tekrar basma debisine bağlı olduğu için her farklı tekrar basma debisi için geç zamanda basınç ve sıcaklık farklı değerlerde sabitlenecektir. Geç zamanlarda doğal beslenme endeksinin rezervuar basıncı üzerinde etkisinin olduğu ama sıcaklık üzerinde etkisinin bulunmadığı görülmüştür.

1. INTRODUCTION

Geothermal energy is heat generated and stored in the earth. The heat is produced primarily by the decay of radionuclides, mostly thorium, uranium and potassium. This heat flux from the earth tends to be strongest along tectonic plate boundaries where volcanic activities are common. Fumaroles, hot springs and mud pots are obvious indications of underground heat, which were used for bathing over the centuries. Bathing and spas have been the oldest and primary uses of geothermal power until the 19th century. Although the geothermal fluids were already being exploited for their energy content in the early 1800s, the main industrial value of geothermal power was understood in 1904, when the first attempt was succeeded at generating electricity from geothermal steam in Lardarello, Italy. Following Italy, Japan, USA and New Zealand were among the countries generating electricity from geothermal power.

Since it did not have to be imported and was economically appropriate compared to other forms of energy, many countries were attracted by geothermal energy after World War 2. Over the years, with the improving technology, geothermal energy utilization has shown a remarkable increase worldwide [url-1].

Geothermal energy is utilized for electricity generation and for other different types of heat direct use applications, e.g. heating purposes, fish farming, bathing, agricultural purposes etc. According to the report by Lund and Boyd (2015) based on country update papers received from 70 countries, the five countries with the largest direct-use (with heat pumps) installed capacity (MW_t) are: China, USA, Sweden, Turkey and Germany accounting for 65.8% of the world capacity. Meanwhile, five countries with the largest annual energy use (with heat pumps) are: China, USA, Sweden, Turkey and Japan accounting for 63.6% of the world use. Figure 1.1 shows the geothermal direct applications worldwide in 2015, distributed by percentage of total installed capacity (MW_t). Accounting for 70.95% of the installed capacity and 55.30% of the annual energy use, geothermal (ground-source) heat pumps have the largest energy use and installed capacity worldwide. The installed capacity of geothermal heat pumps is 49898 MW_t and the annual energy use is 325028 TJ/yr (Lund and Boyd, 2015).

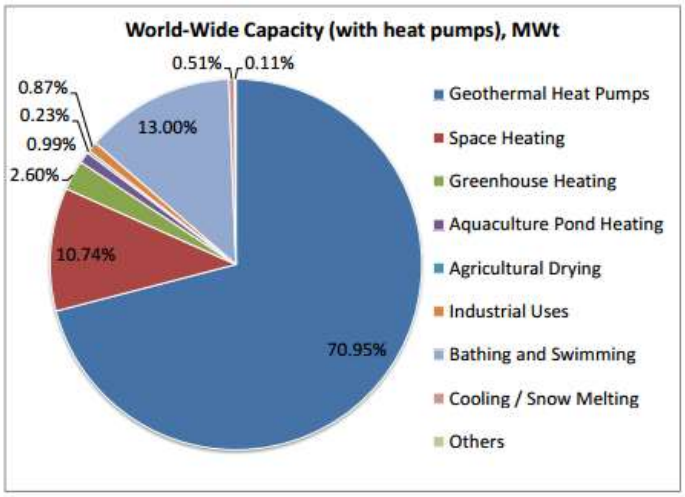

Figure 1.1 : Geothermal direct applications worldwide in 2015, distributed by percentage of total installed capacity (MW_t).

Main utilization type of geothermal energy is generating electricity from hydrothermal resources. Since it is renewable, safe and sustainable, countries tend to increase the number of power plants. Figure 1.2 shows the international installed geothermal power capacity.

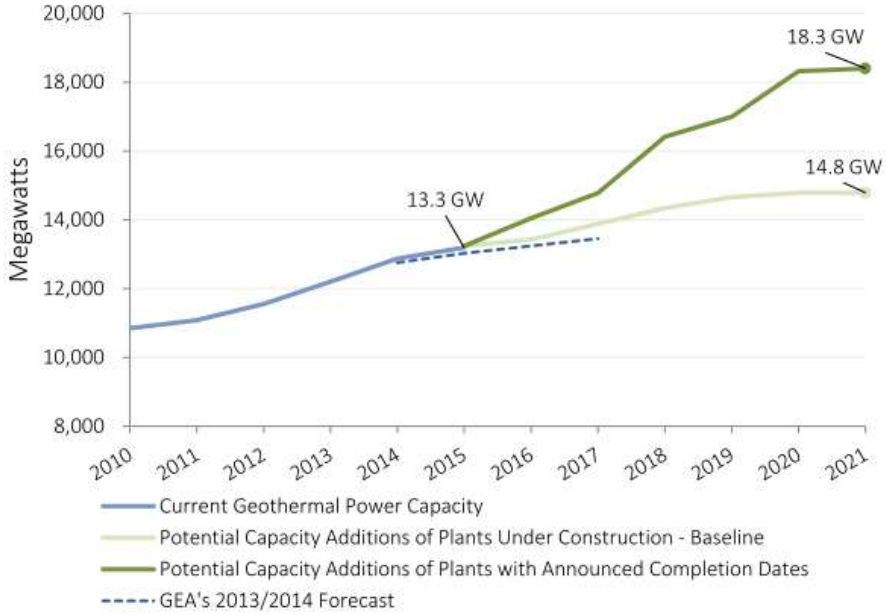

Figure 1.2 : International Geothermal Power Nameplate Capacity (MW_e).

According to Antics et.al. (2016), Italy is the leading country in Europe with the installed geothermal power capacity of 916 MW_e, followed by Iceland with that of 661 MW_e. The same source states that Turkey is the third country in Europe with the installed capacity of 650.2 MW_e. Figure 1.3 lists the Europe countries based on the installed geothermal power generation capacity by 2015. According to the updated reports, Italy is the first country in Europe with installed power capacity of 944 MW_e and Turkey is the second country with that of 775 MW_e as of December 2016 (Personal communication with Prof. Dr. Abdurrahman SATMAN).

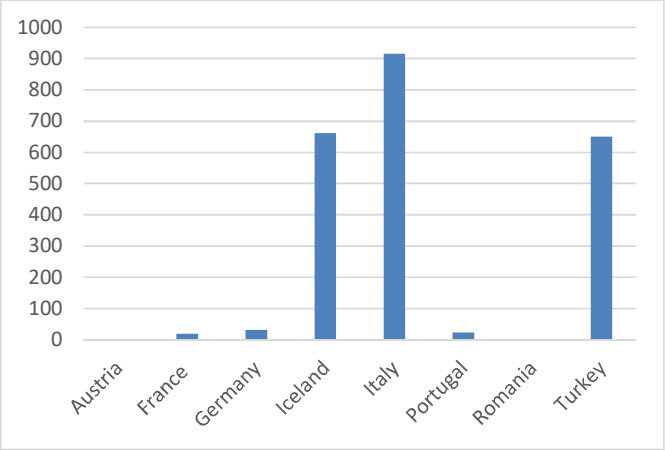

Figure 1.3 : Installed Geothermal Power Capacity (MW_e) in Europe in 2015.

Being environmentally friendly competitive to other energy types is another reason why countries support geothermal energy. Because geothermal power plants do not burn fuel to produce electricity, their emission levels are very low. According to Holm et.al. (2012), geothermal plants emit about 5% of the carbon dioxide, 1% of the sulfur dioxide, and less than 1% of the nitrous oxide emitted by a coal-fired plant of equal size, and certain types of geothermal plants produce near-zero emissions.

1.1. Literature Review

A reservoir model is a utility describing the change in reservoir pressure and temperature as a function of time or cumulative fluid production. Similar to oil reservoir modelling, pressure and temperature are the main parameters to consider when modelling the geothermal reservoirs. Primary objectives of geothermal reservoir modeling are to estimate production capacity of the geothermal fields, the rate of

reservoir pressure decline and the effects of fluid recharge and injection on field performance. There are mainly three methods of modeling available in the literature, which are decline curve analysis, numerical modeling and lumped parameter modeling.

Like in the oil and gas reservoirs, loss of reservoir pressure is usually the reason why geothermal fluid production rate declines as a function of time. In order to analyze well production data to forecast production decline rates in geothermal wells decline curve method is used. Decline curve analysis is a graphical procedure used to forecast future well performance by analyzing this declining production rate.

In numerical models, the reservoir is simulated with many number of gridblocks. This model studies the geothermal reservoir behavior by solving the mass and energy balance equations. Since all mathematics required to solve the resulting equations are included in the background of the tool, it allows to simulate the whole reservoir with heterogeneities and to understand the hydrogeological behavior and heat transport in the reservoir. However, the disadvantage of this modeling is that it requires an extensive amount of data about the reservoir and much more run times compared to other modeling methods. (Tureyen et. al., 2009)

Lumped parameter model is known as zero dimensional model. Since this model represents the geothermal system as a group of tanks, it is also called tank models. Tank model is considered as a highly simplified form of the numerical modeling. It consists of homogenous tanks which are parametrized with a few average parameters. Each tank represents the reservoir and/or the recharge source. Because it requires a few averaged parameters, it is reasonable to use this method in the early life of the field when there is less data available. (Sarak, 2004).

Several lumped parameter models have been proposed in the literature, some of which have been successfully used to simulate data from well known geothermal fields. Whiting and Ramey (1969) were the first to use this concept to model the Wairakei reservoir in New Zealand. Their non-isothermal tank model included both mass and energy balance equations considering conduction and convection terms. The model was valid for both single phase and two phase systems. However, in this model

variable rate production/injection scenario was not considered and the model ignored the non-isothermal effects for reservoirs containing only compressed liquid water.

Brigham and Morrow (1974) developed three models valid for closed, vapor-dominated reservoirs. Brigham and Neri (1980) modeled the Gabbro zone of the Larderello field.

Castanier et al. (1980), and Castanier and Brigham (1983) proposed an analytical model for simulation of geothermal reservoirs which can be applied to any type of geothermal reservoirs such as all liquid, all steam or two phase.

Some examples of lumped parameter models assuming isothermal flow behavior can be found in the literature. Models proposed by Grant et al. (1982), Axelsson (1989), Sarak et al. (2005), Alkan and Satman (1990) and Tureyen et al. (2007) are isothermal flow behavior models. Assuming the system is isothermal, one can model the field pressure to a certain degree, ignoring the temperature change. However, temperature change could play an important role when there are reinjection operations in a field or when the recharge temperature is considerably different from the reservoir temperature. Onur et al. (2008) has developed a non-isothermal lumped parameter model for liquid dominated geothermal reservois.

The model proposed by Onur et al. (2008) account for variable rate non-isothermal flow which incorporates both mass and energy balance equations considering only convection. This model is used to predict both pressure and temperature behavior of a single phase liquid-dominated geothermal reservoirs. Onur et al. (2008) show that reservoir parameters such as bulk volume and porosity can be determined by using temperature data together with pressure data in history-matching, referring to the fact that those parameters can not be obtained from pressure data alone by using an isothermal model.

To model the effects of aquifers and reservoirs in hydraulic communication, Tureyen et al. (2009) extended the model of Onur et al. (2008) to multiple tanks. This model lacked the effects of heat conduction. Tureyen and Akyapi (2010) generalized the

model of Onur et al., (2008) and Tureyen et al., (2009) to consider the effects of heat conduction.

1.2. Statement of Problem

Most of the models proposed above are valid for geothermal reservoirs under constant flow rate production scenario. When geothermal reservoirs are considered, it becomes crucial to produce at a constant energy rate either for power plants or for direct use at a specified installed capacity. When modeling is considered at a fixed flow rate, this could lead to misleading future predictions in cases where the temperature of the reservoir changes. Hence, it would become very useful to be able to perform modeling based on a constant energy rate production scheme. The main objectives of this thesis is to discuss the differences between the geothermal reservoir performances under constant rate production and constant energy production schemes and to see the effects of some parameters on reservoir pressure and temperature under constant energy production sceme.

Description of new mathematical model used in this thesis will be discussed in Chapter 2. Chapter 3 includes the modeling study done with the new model. The effects of various parameters on the performance behavior of liquid dominated geothermal reservoirs under constant energy production scenario are discussed in Chapter 3. Conclusions will be explained in Chapter 4.

2. LUMPED PARAMETER MODELING

Since lumped parameter modeling requires much less data and time compared to numerical modeling, it is a good alternative to model the pressure and temperature profile of the reservoir especially at the early life of the field. Grant et al. (1982), Axelsson (1989), Sarak et al. (2005), and Tureyen et al. (2007) have previously modeled pressure behavior of a low-temperature geothermal reservoirs. These models assume that the reservoir can be treated as an isothermal system. This assumption means that pressure profile of the reservoir can be modeled, but the changes in the temperature will be ignored. However, temperature changes can play an important role when there are reinjection operations in a field or when the recharge temperature is significantly different than the reservoir temperature. The average reservoir temperature depends on reservoir volume, production rate, reinjection rate, reinjection temperature, natural recharge rate and the natural recharge temperature. In this chapter, we will use a non-isothermal tank model which will account for the temperature changes as well.

2.1. Non-Isothermal Lumped Parameter Model

The mathematical background of the new non-isothermal lumped parameter model will be explained in this section. The model developed in this thesis is based on the conservation of mass and conservation of energy for a single phase fluid (water). Schematic view of a single tank open system is illustrated in Fig. 2.1.

As illustrated in Fig. 2.1, the geothermal system is considered as a single tank. The tank has a bulk volume V_b, temperature T, pressure p and porosity ϕ. w_p (kg/s) represents the production rate and w_i (kg/s) represents the injection rate of water in to the reservoir. The bulk volume and the porosity of the tank is assumed to be constant.

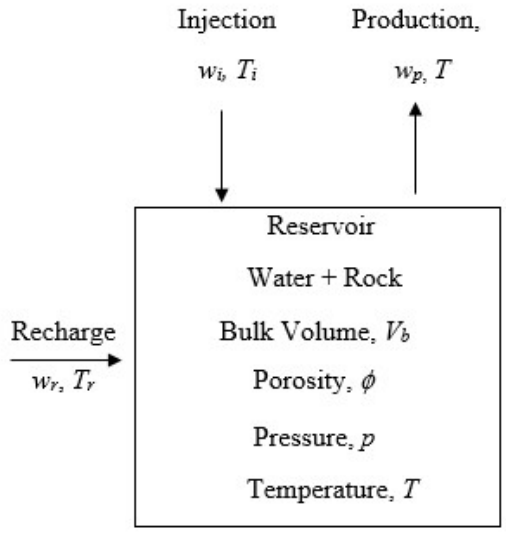

Figure 2.1 : Schematic of a single tank open system.

Where as the pressure and the temperature change with time. Hence the net production rate w_{net} (kg/s) can be defined as:

$$w_{net} = w_p - w_i \tag{2.1}$$

Fluid flow will take place from the recharge source in to the reservoir due to the production from the tank. In this study, the steady-state Schilthuis (1936) water influx method is used to describe the recharge rate between the recharge source and the reservoir. According to Schilthuis (1936) the recharge rate, w_r (kg/s) is proportional to the pressure difference between the recharge source and the reservoir and can be defined as:

$$w_r = \alpha[p_r - p(t)] \tag{2.2}$$

Where α (kg/bar-s) is the reservoir recharge constant, p_r (bar) is the pressure of the recharge source and $p(t)$ (bar) represents the pressure of the reservoir as a function of time.

2.1.1. Conservation of mass

The mass balance equation for the tank illustrated above can be written as:

$$\left(\begin{array}{c}\text{Accumulation rate}\\ \text{of mass in}\\ \text{control volume}\end{array}\right) = \left(\begin{array}{c}\text{Mass rate}\\ \text{from recharge}\end{array}\right) + \left(\begin{array}{c}\text{Mass rate}\\ \text{from injection}\end{array}\right) - \left(\begin{array}{c}\text{Mass rate}\\ \text{from production}\end{array}\right) \tag{2.3}$$

$$w_{acc} = w_r + w_i - w_p \tag{2.4}$$

where w_{acc} (kg/s) is the liquid mass accumulation and is defined as:

$$w_{acc} = \frac{\partial\left(V_b \phi \rho_w\right)}{\partial t} \tag{2.5}$$

where ρ_w (kg/m^3) is the liquid density and t is time (s).

Hence, equation 2.4 becomes:

$$\frac{\partial\left(V_b \phi \rho_w\right)}{\partial t} = w_r + w_i - w_p \tag{2.6}$$

Assuming the bulk volume is constant, then equation 2.6 becomes:

$$V_b\left(\rho_w \frac{\partial \phi}{\partial t} + \phi \frac{\partial \rho_w}{\partial t}\right) = w_r + w_i - w_p \tag{2.7}$$

Using the chain rule and the compressibilities of rock and fluid, Equation 2.7 becomes;

$$V_b \rho_w \phi c_t \frac{\partial p}{\partial t} = w_r + w_i - w_p \tag{2.8}$$

where c_t (bar^{-1}) is the total compressibility and is defined as;

$$c_t = c_w + c_{ro} \tag{2.9}$$

where c_w (bar^{-1}) is the water compressibility and c_{ro} (bar^{-1}) is the rock compressibility.

When the Schilthuis approach is used to model the recharge rate;

$$V_b \rho_w \phi c_t \frac{\partial p}{\partial t} = \alpha\left[p_r - p(t)\right] + w_i - w_p \tag{2.10}$$

Let;

$$V_b \rho_w \phi c_t = \kappa \tag{2.11}$$

where κ (kg/bar) is the storage capacity and represents the amount of mass of the fluid which can expand in a unit pressure drop.

If we define

$$\Delta p = p_r - p(t) \tag{2.12}$$

Then;

$$\frac{d\Delta p}{dt} = -\frac{dp}{dt} \tag{2.13}$$

Replacing these definitions in Equation 2.10 and rearranging gives;

$$-\kappa\frac{d\Delta p}{dt} = \alpha\Delta p - w_{net} \tag{2.14}$$

Rearranging the equation above, we get;

$$-\kappa\frac{d\Delta p}{dt} - \alpha\Delta p + w_{net} = 0 \tag{2.15}$$

The equation is a first order ordinary differential equation which has a solution given by;

$$\Delta p = \frac{w_{net}}{\alpha} - \frac{\left(w_{net} - \alpha\Delta p_0\right)}{\alpha} e^{-\alpha\frac{t}{\kappa}} \tag{2.16}$$

$$\Delta p_0 = p_r - p_0 \tag{2.17}$$

where Δp_0 (bar) is the pressure difference between the recharge source and the reservoir at initial time.

Rearranging the equation 2.16 yields;

$$\Delta p = \frac{w_{net}}{\alpha}\left[1 - e^{-\alpha\frac{t}{\kappa}}\right] + \Delta p_0 e^{-\alpha\frac{t}{\kappa}} \tag{2.18}$$

For the late time behavior of the reservoir, the exponential term in equation 2.18 can be approximated by $e^{-\frac{\alpha t}{\kappa}} \cong 0$, when time is treated large enough. Hence, the pressure solution in equation 2.18 reduces to;

$$\Delta p_{ss} \cong \frac{w_{net}}{\alpha} \tag{2.19}$$

Equation 2.19 indicates that at late time the reservoir pressure stabilizes at an equilibrium value determined by the net production rate. The pressure decline at late time becomes independent of the reservoir storage coefficient, κ and bulk volume, V_b.

For constant flow rate production scenario, steady state pressure drop will be;

$$\Delta p_{ss} \cong \frac{w_{net}}{\alpha} \cong \frac{w_p - w_i}{\alpha} \tag{2.20}$$

Now we will consider the constant energy production scenario. As expected, since the temperature decreases by the mass production from the reservoir, the flow rate needs to be increased with time to provide the constant energy production. Energy produced from the geothermal power plants can be defined as:

$$e_p = e_{th}\eta \tag{2.21}$$

where e_p (MW_e) is the produced energy from the power plant, e_{th} (MW_t) is the thermal energy of the produced water going in to the power plant and η (fraction) is the conversion efficiency of the power plant from thermal energy to electrical energy.

Here the thermal energy of the produced water, e_t, can be approximated by;

$$e_{th} = w_p C_{wp} T \tag{2.22}$$

Substituting equation 2.22 into equation 2.21 and rearranging, we get the production rate as;

$$w_p = \frac{e_p}{C_{wp} T \eta} \tag{2.23}$$

For constant energy production scenario, using equation 2.23 in equation 2.19, steady state pressure drop will be,

$$\Delta p_{ss} \cong \frac{w_{net}}{\alpha} \cong \frac{w_p - w_i}{\alpha} \cong \frac{e_p}{C_{wp} T_{ss} \eta \alpha} - \frac{w_i}{\alpha} \tag{2.24}$$

Or assuming that the injection rate is some fraction of the production rate, which is generally the case in this study;

$$w_i = x w_p \tag{2.25}$$

where x is the reinjection ratio.

The steady state pressure drop equation becomes;

$$\Delta p_{ss} \cong \frac{w_{net}}{\alpha} \cong \frac{w_p - w_i}{\alpha} \cong \frac{(1-x)w_p}{\alpha} \cong \frac{(1-x)e_p}{C_{wp}T_{ss}\eta\alpha} \tag{2.26}$$

2.1.2. Conservation of energy

In geothermal systems, it is usually the convection that dominates the heat transfer process. In other words, the temperature changes occur mostly because of fluid movement such as production, reinjection or flow from the recharge source. The energy balance equation for the tank illustrated in Fig. 2.1 can be written as:

$$\begin{pmatrix}\text{Accumulation}\\ \text{of energy in}\\ \text{control volume}\end{pmatrix} = \begin{pmatrix}\text{Heat flow}\\ \text{from recharge}\end{pmatrix} + \begin{pmatrix}\text{Heat flow}\\ \text{from injection}\end{pmatrix} - \begin{pmatrix}\text{Heat flow}\\ \text{from production}\end{pmatrix} \tag{2.27}$$

Note that heat transfer due to conduction and heat losses to the surroundings are neglected. When the conservation of energy is applied to the tank in Fig. 2.1, we get;

$$V_b \frac{d}{dt}\left[(1-\phi)\rho_{ro}C_{ro}T + \phi\rho_w u_w\right] = -w_p h_w + w_i h_i + w_r h_r \tag{2.28}$$

where, C_{ro} (J/kg-^{0}C) defines the specific heat capacity of the rock matrix, u_w (J/kg) is the specific internal energy of water, h_w (J/kg) is the specific enthalpy of the produced water, h_i (J/kg) is the specific enthalpy of the injected water, h_r (J/kg) is the specific enthalpy of the recharge source water, α (kg/bar-s) is the recharge index between the recharge source and the reservoir, ρ_w (kg/m^3) is the water density, and ρ_{ro} (kg/m^3) is the rock density.

We can make the following approximations;

$$u_w = h_w = C_{wp}T \tag{2.29}$$

$$h_i = C_{wi}T_i \tag{2.30}$$

$$h_r = C_{wr}T_r \tag{2.31}$$

where C_{wp} (J/kg-^{0}C) is the specific heat capacity of the produced water, C_{wi} (J/kg-^{0}C) is the specific heat capacity of the injected water and C_{wr} (J/kg-^{0}C) is the specific heat capacity of the rechare source water.

Replacing these definitions into equation 2.28 gives;

$$V_b \frac{d}{dt}\left[(1-\phi)\rho_{ro} C_{ro} T + \phi\rho_w C_w T\right] = -w_p C_{wp} T + w_i C_{wi} T_i + w_r C_{wr} T_r \tag{2.32}$$

$$V_b\left[(1-\phi)\rho_{ro} C_{ro} T + \phi\rho_w C_w T\right]\frac{dT}{dt} = -w_p C_{wp} T + w_i C_{wi} T_i + w_r C_{wr} T_r \tag{2.33}$$

Let;

$$V_b\left[(1-\phi)\rho_{ro} C_{ro} T + \phi\rho_w C_w T\right] = \gamma \tag{2.34}$$

then equation 2.33 becomes;

$$\gamma \frac{dT}{dt} = -w_p C_{wp} T + w_i C_{wi} T_i + w_r C_{wr} T_r \tag{2.35}$$

Substituting equations 2.2 and 2.18 into equation 2.35 and rearranging gives;

$$\gamma \frac{dT}{dt} + w_p C_{wp} T - w_i C_{wi} T_i - w_{net} C_{wr} T_r + w_{net} C_{wr} T_r e^{-\alpha \frac{t}{\kappa}} - \Delta p_0 \alpha C_{wr} T_r e^{-\alpha \frac{t}{\kappa}} = 0 \tag{2.36}$$

Equation 2.36 is a linear first order ordinary differential equation with the solution;

$$T(t) = \frac{\Delta p_0 \alpha C_{wr} T_r - w_{net} C_{wr} T_r}{w_p C_{wp} - \gamma \frac{\alpha}{\kappa}} e^{-\alpha \frac{t}{\kappa}} + \frac{w_i C_{wi} T_i + w_{net} C_{wr} T_r}{w_p C_{wp}} +$$

$$+ \left[T_0 + \frac{w_{net} C_{wr} T_r - \Delta p_0 \alpha C_{wr} T_r}{w_p C_{wp} - \gamma \frac{\alpha}{\kappa}} - \frac{w_i C_{wi} T_i + w_{net} C_{wr} T_r}{w_p C_{wp}} \right] e^{-\left(\frac{wpCwp}{\gamma} t\right)} \tag{2.37}$$

For the late time behavior of the reservoir, the exponential terms in equation 2.37 can be approximated by $e^{-\left(\frac{wpCwp}{\gamma} t\right)} \cong 0$ and $e^{-\alpha \frac{t}{\kappa}} \cong 0$ when time is treated large enough.

Thus, the temperature solution in equation 2.37 reduces to;

$$T_{ss} \cong \frac{w_i C_{wi} T_i + w_{net} C_{wr} T_r}{w_p C_{wp}} \tag{2.38}$$

Considering equation 2.25, when injection rate is some fraction of the production rate, steady state temperature reduces to;

$$T_{ss} \cong \frac{w_i C_{wi} T_i + w_{net} C_{wr} T_r}{w_p C_{wp}} \cong \frac{x w_p C_{wi} T_i + (w_p - x w_p) C_{wr} T_r}{w_p C_{wp}} \cong \frac{x C_{wi} T_i + (1-x) C_{wr} T_r}{C_{wp}} \tag{2.39}$$

From equation 2.39, it is clear that when the injection rate is some fraction of the production rate, steady state temperature is independent of the production rate. Hence, steady state temperature should be same for constant flow rate and constant energy production scenarios, no matter the production rate is constant or increasing.

2.1.3. Constant energy production

The pressure and temperature equations developed in the previous subsections have been derived under the assumption of constant production mass rate. In order to perform production at a constant energy rate, the total production time is split into small time steps and the equations given in the previous time steps are applied. Of course, within these small time intervals the production rate is assumed to be constant. The following algorithm shown in Fig. 2.2 is applied for constant energy production.

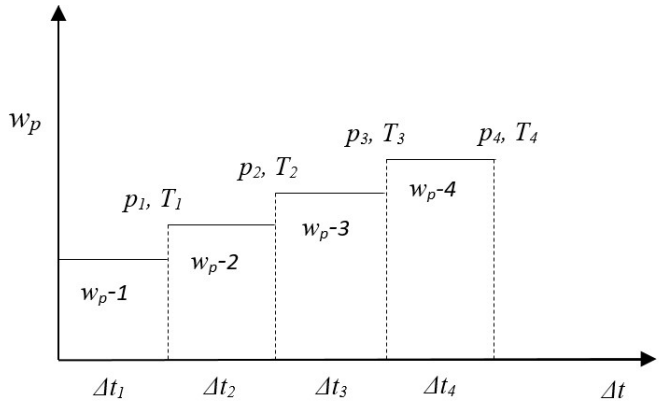

Figure 2.2 : Algorithm of the non-isothermal lumped parameter model for constant energy production.

1) Choose a small time step Δt and compute the initial flow rate to be used using Equation 2.23.

2) Assuming a constant flow rate compute the pressure and temperature at the end of the Δt time period using Equations 2.18 and 2.37 respectively.

3) Select a new time interval Δt and repeat the above time steps until the end time is reached.

3. MODELING STUDY

This chapter includes several runs comparing the geothermal reservoir behavior under constant flow rate production scheme and constant energy production scheme. Reservoir pressure and temperature are the benchmarks for comparison. The other objective of this chapter is to observe the effects of several parameters on the geothermal reservoir performance under constant energy production scenario.

Consider the model of a geothermal system shown in Fig. 2.1, consisting of a reservoir and a recharge source. The system is in equilibrium at initial time, $t=0$. For the base case, the bulk volume of the reservoir is $V_b=10^8$ m^3. The reservoir is produced at a mass rate of w_p and the recharge source at a constant pressure of p_r, supplies the water recharge. The recharge constant between the reservoir and the recharge source is assumed to be α=10 kg/bar-s. The reservoir is planned to flow 20000 days and energy production, e_p is assumed to be 50 MW$_e$ and the porosity ϕ is assumed to be 0.05. Injection rate, w_i is assumed to be 80% of the production rate and the conversion efficiency of the power plant, which is defined as η, is assumed to be 0.15. Although conversion efficiency is expected to change with temperature, it will still be assumed as constant for simplicity even in the higher temperature changes. Pressure, p and temperature, T are the benchmarks to be compared for both constant energy production and constant flow rate production scenarios. The assumed geothermal reservoir parameters are listed in Table 3.1.

Table 3.1 : Parameters used in the model.

V_b (m^3)	1.00E+08	**C_{wr} (J/kg-^{o}C)**	4344.6
ϕ (fraction)	0.05	**c_{ro} (bar^{-1})**	1.00E-04
α (kg/bar-s)	10	**c_w (bar^{-1})**	1.28E-04
ρ_{ro} (kg/m^3)	2600	**c_t (bar^{-1})**	2.28E-04
ρ_w (kg/m^3)	811.41	**T_i (^{o}C)**	100
C_{ro} (J/kg-^{o}C)	1000	**T_r (^{o}C)**	250
C_w (J/kg-^{o}C)	4344.6	**T_0 (^{o}C)**	250
C_{wi} (J/kg-^{o}C)	4302.7	**P_0 (bar)**	150

Five hypothetical cases of one tank model will be proposed and analysed to study reservoir pressure and temperature behavior under constant flow rate production and constant energy production scenarios. In each case, all parameters will be kept same as in the base case and only one parameter will be changed to see its effect on the reservoir performance behavior. The changing parameters will be bulk volume, installed power capacity, porosity, reinjection ratio and reservoir recharge constant.

All cases will be studied under two scenarios:

Scenario 1: Constant flow rate production

Scenario 2: Constant energy production.

Base Case

In the base case, $V_b = 10^8$ m^3, $e_p = 50$ MW$_e$, $\phi = 0.05$, $w_i = 0.8 \text{x} w_p$, $\alpha = 10$ kg/bar-s. All parameters are given as input to the model and reservoir performance for 20000 days is predicted. The figures below show the temperature, pressure and production rate behaviors of the reservoir for the base case.

Fig. 3.1 shows the comparison of the reservoir temperature profiles under constant flow rate and constant energy production scenarios. From the graph shown in Fig. 3.1, it is obvious that the reservoir temperature has reached its steady state after 10000 days. It is also observed that steady state temperature is the same for both scenarios. From the previous chapter we know that steady state temperature is not dependent on the production rate, in case the injection rate is some fraction of the production rate.

From equation **2.39**, steady state temperature is calculated as;

$$T_{ss} \cong \frac{0.8C_{wi}T_i + 0.2C_{wr}T_r}{C_{wp}} \cong \frac{0.8x4302.7x100 + 0.2x4344.6x250}{4273} \cong 131.2\,^0\text{C}$$

As shown in the calculation above, since temperature at late time is independent of the production rate, it stabilizes at the same value under both scenarios, no matter the flow rate is constant or increasing.

Note that specific heat capacity of the produced water, C_{wp} at late time approximates to 4273 J/kg-^{0}C.

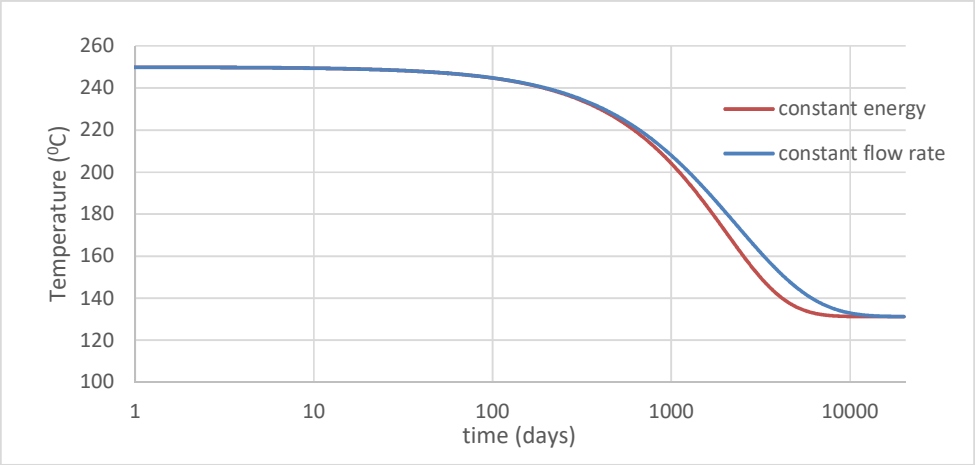

Figure 3.1 : Comparison of temperature profiles under constant flow rate production and constant energy production scenarios.

Fig. 3.2 shows the change of flow rate with time for constant energy production scheme. Since reservoir fluid temperature declines with the production from the tank, the flow rate needs to be increased with time to supply the constant energy production. As expected, when the temperature reaches the steady state and behave almost constant, the flow rate will also be constant. In other words, steady state flow rate can be defined as the flow rate at the time that temperature reaches to steady state.

From Equation 2.23, we calculate initial flow rate and steady state flow rate as:

$$w_p = \frac{50x10^6}{4344.6x250x0.15} = 307\,\text{kg/s}$$

$$w_{p\_ss} = \frac{e_p}{C_{wp}T_{ss}\eta} = \frac{50x10^6}{4273x131.2x0.15} = 595\ \text{kg/s}$$

It means that to produce constant energy of 50 MW_e, the flow rate will start with 307 kg/s at initial time and will increase with time as the temperature decreases. When the temperature reaches the steady state, the flow rate will reach to 595 kg/s and be almost constant since that time. As equation indicates, at late time flow rate production depends on the steady state temperature and specific heat capacity of the produced water. Since temperature and specific heat capacity of the produced water stabilizes at some value at late time, flow rate production will also stabilize at an equilibrium value determined by equation 2.23.

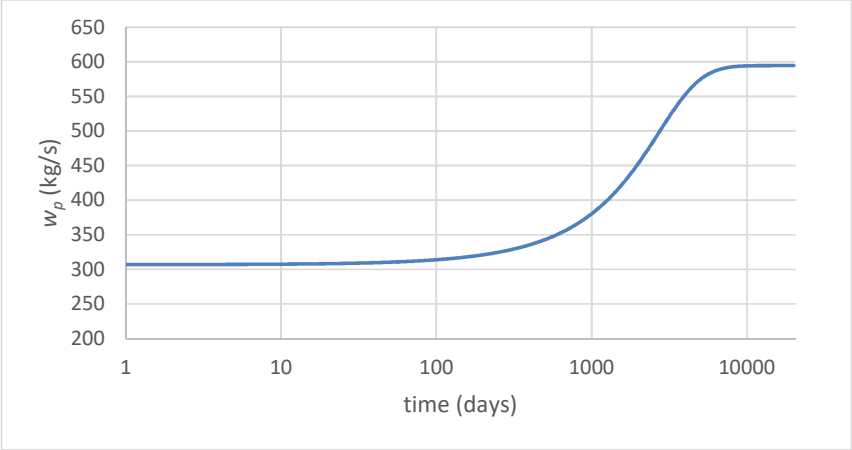

Figure 3.2 : Change of flow rate production with time under constant energy production scenario.

The comparison of reservoir pressure behaviors for the base case is shown in Fig. 3.3. As it is seen, reservoir pressure stabilized at the very early time when it flows under constant flow rate production scenario. However, the pressure stabilizes after almost 10000 days when it flows under constant energy production scenario and steady state pressures are different in each scenario. Because steady state pressure drop is dependent on the net flow rate, it is reasonable that steady state pressures be different under constant flow rate and constant energy production scenarios. Calculations are shown below.

In the base case, injection rate is 80% of the production rate. Therefore, from the equation 2.1, the net production rate is;

$$w_{net} = w_p - w_i = w_p - 0.8w_p = 0.2w_p$$

Because recharge constant in this case is α=10 kg/s, from equation 2.19 the steady state pressure drop is calculated as;

$$\Delta p_{ss} \cong \frac{0.2w_p}{\alpha} \cong 0.02w_p \tag{3.1}$$

For constant flow rate production scenario, flow rate production is calculated from equation 2.23;

$$w_p = \frac{50x10^6}{4344.6x250x0.15} = 307\,\text{kg/s}$$

Equation 3.1 gives steady state pressure drop for constant flow rate production as;

$$\Delta p_{ss} \cong 0.02 w_p = 0.02x307 \cong 6.14 \text{ bar}$$

$$p_{ss} \cong p_0 - \Delta p_{ss} \cong 150 - 6.14 \cong 143.86 \text{ bar}$$

For constant energy production scenario, substituting equation 2.23 into equation 3.1, steady state pressure drop will be,

$$\Delta p_{ss} \cong 0.02 \frac{e_p}{C_{wp} T_{ss} \eta} \cong \frac{0.02x50x10^6}{4273x131.2x0.15} \cong 11.89 \text{ bar}$$

$$p_{ss} \cong p_0 - \Delta p_{ss} \cong 150 - 11.89 \cong 138.11 \text{ bar}$$

An interesting point in Fig. 3.3 is that there are two pressure stabilizations under constant energy production scenario which are at early time and late time periods. This is actually directly related to reservoir temperature behavior. To see the obvious relationship between temperature, flow rate and pressure, they are plotted on Fig. 3.4. We know that the temperature has reached the steady state regime after 10000 days. Hence, the second pressure stabilization is actually the steady state pressure of the reservoir. However, when analyzing temperature profile in Fig. 3.4, it is seen that at early time period the temperature change is so small that it can be regarded as constant. Since temperature is constant, the flow rate should be kept constant as well to maintain the energy production constant. Since pressure drop is dependent on the net flow rate, the pressure will behave as constant when the flow rate is kept constant. Therefore, the first plateau in the pressure profile in Fig 3.3 is due to the small temperature change of the reservoir.

First Case

In the first case, e_p = 50 MW_e, ϕ = 0.05, w_i = 0.8xw_p, α = 10 kg/bar-s. The changing parameter is V_b. The e_p, ϕ, w_i, α and other reservoir parameters are fed into the model to regenerate the pressure and temperature behavior over 20000 days. Model has been

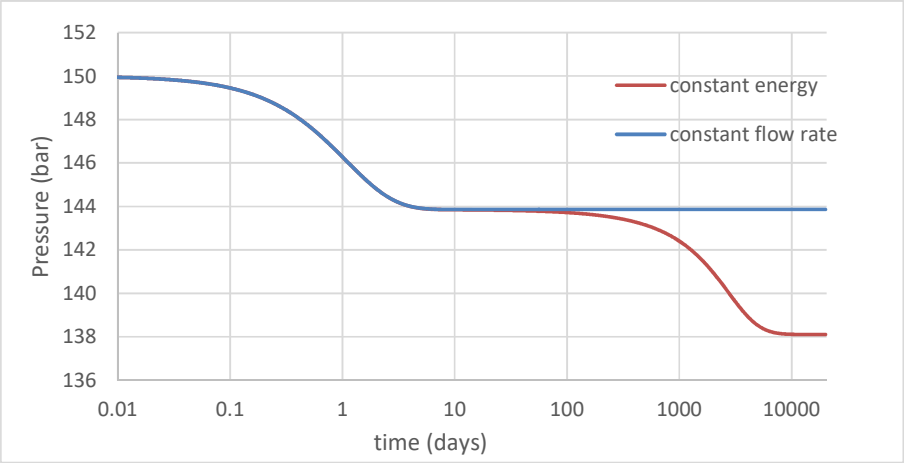

Figure 3.3 : Comparison of pressure profiles under constant flow rate production and constant energy production scenarios.

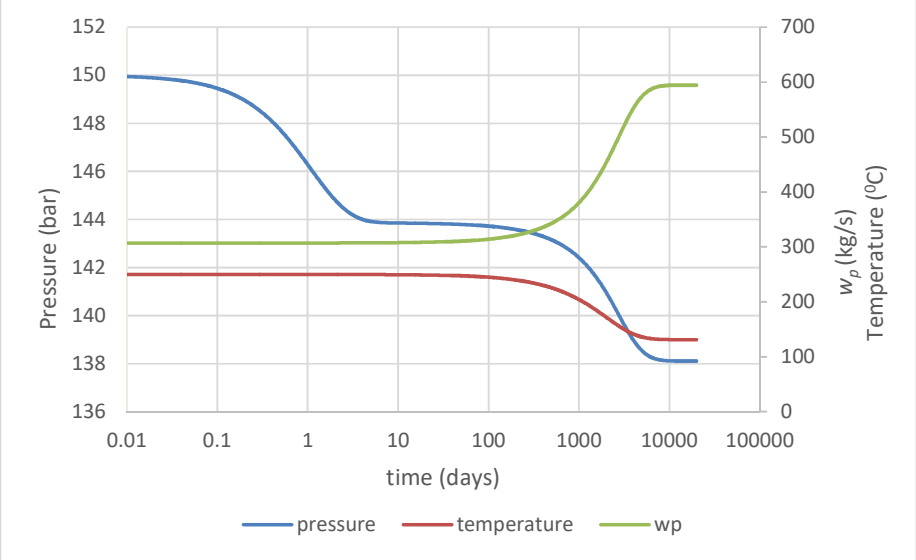

Figure 3.4 : Temperature, pressure and flow rate profiles under constant energy production scenario.

run four times for various bulk volumes of $V_b = 10^7$ m^3, $V_b = 10^8$ m^3, $V_b = 10^9$ m^3 and $V_b = 10^{10}$ m^3.

The pressure and temperature profile of the reservoir for various bulk volumes over 20000 days under constant flow rate production and constant energy production scenarios are shown in figures below. Fig. 3.5 and Fig. 3.6 show that temperature at late time is observed to stabilize at the same value for various bulk volumes under

both scenarios. In order to explain this case, we need to look at the formulas for late time.

Let's recall the temperature solution we derived in Chapter 2. Equation 2.39 shows that steady state temperature is independent of bulk volume, but depends on the specific heat capacity of the produced water, C_{wp}. As noted above, specific heat capacity of water C_{wp} at late time approximates to 4273 J/kg-^{0}C.

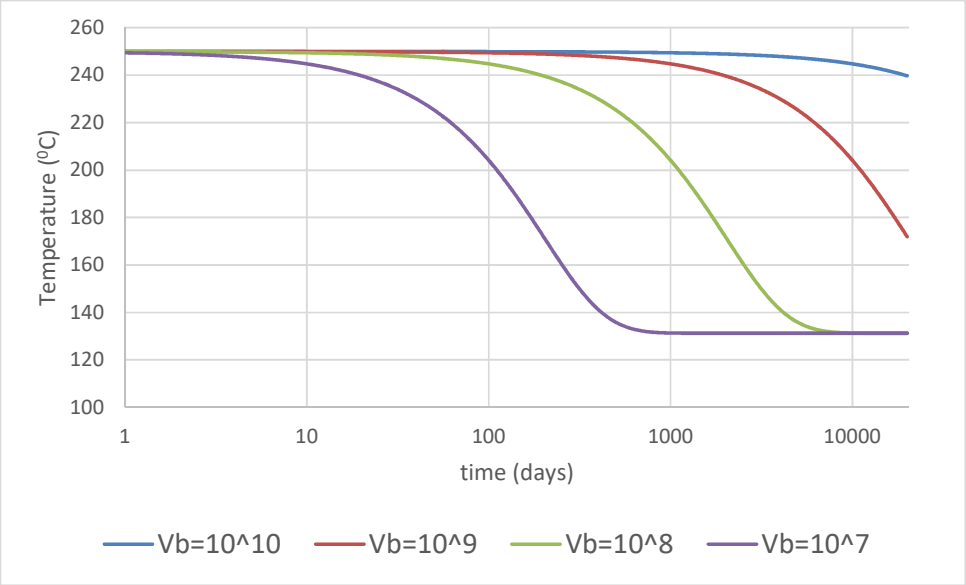

Figure 3.5 : Comparison of temperature behavior for various bulk volumes under constant energy production scenario.

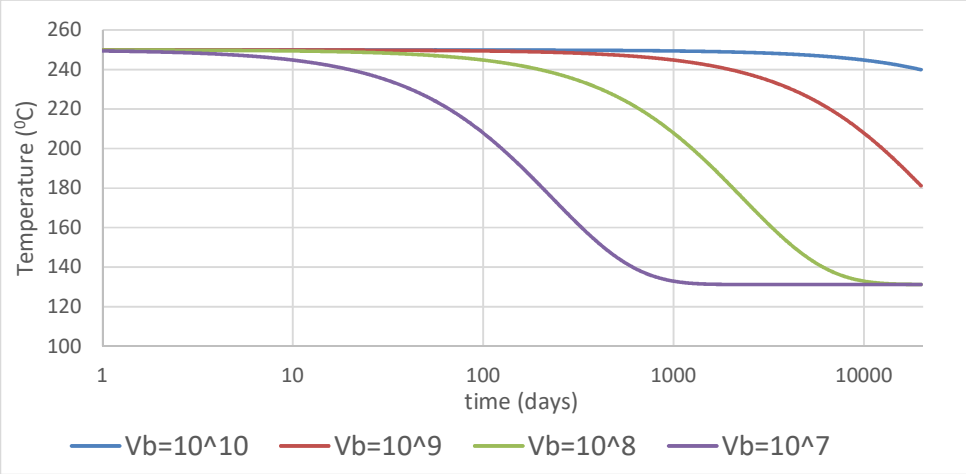

Figure 3.6 : Comparison of temperature behavior for various bulk volumes under constant flow rate production scenario.

Thus, from the temperature solution in equation 2.39, for all bulk volumes late time temperature will be calculated as;

$$T_{ss} \cong \frac{0.8C_{wi}T_i + 0.2C_{wr}T_r}{C_{wp}} \cong \frac{0.8x4302.7x100 + 0.2x4344.6x250}{4273} \cong 131.2\,^0\text{C}$$

Since C_{wi}, C_{wr}, T_i and T_r are constant, it is obvious that T_{ss} will be dependent only on C_{wp}. Because C_{wp} also stabilizes at some value at late time, then the late time temperature in all cases will stabilize at approximately 131.2 ^{0}C, being independent of bulk volume and regardless of constant energy production and constant flow rate production scenarios.

Another observation in temperature profiles is that reservoir temperatures reach steady states at different times for various bulk volumes. This is actually as expected, smaller the bulk volume, later the stabilization time for reservoir temperature.

Fig. 3.7 shows that flow rate productions for various bulk volumes also stabilize at the same value at late time. The initial flow rate and steady state flow rate are calculated as in the base case.

$$w_p = \frac{50x10^6}{4344.6x250x0.15} = 307\ \text{kg/s}$$

$$w_{p\_ss} = \frac{e_p}{C_{wp}T_{ss}\eta} = \frac{50x10^6}{4273x131.2x0.15} = 595\ \text{kg/s}$$

As equation indicates, flow rate production at late time does not depend on bulk volume when constant energy production is considered. Because stabilization time for temperatures for various bulk volumes under constant energy production scheme is different, stabilization time for flow rates will be different as well.

Fig. 3.8 and Fig. 3.9 show that pressure curves for various bulk volumes display the same trend and the pressures at late time stabilize at the same value. However, steady state pressures are different in each scenario.

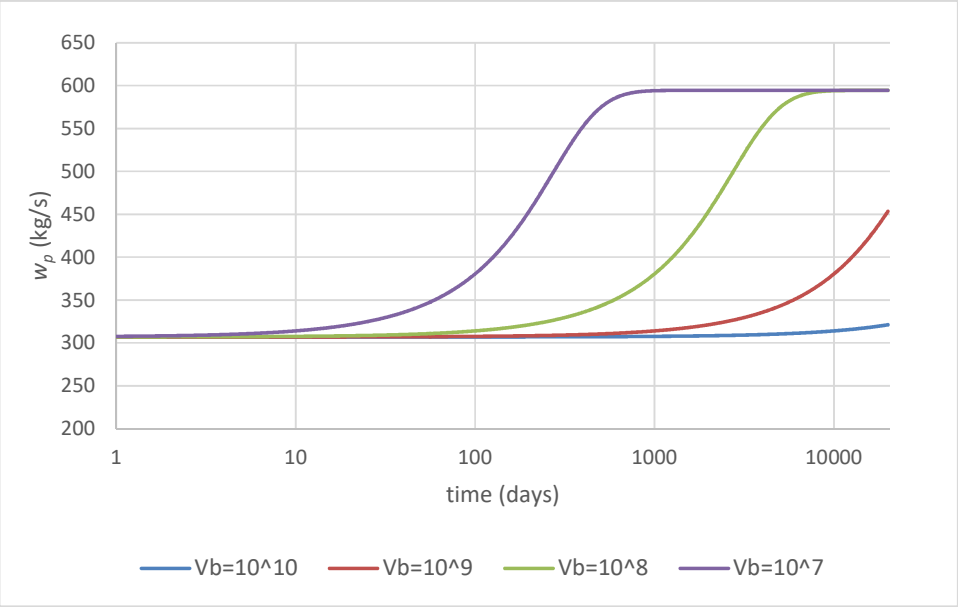

Figure 3.7 : Change of flow rate productions with time for various bulk volumes under constant energy production scenario.

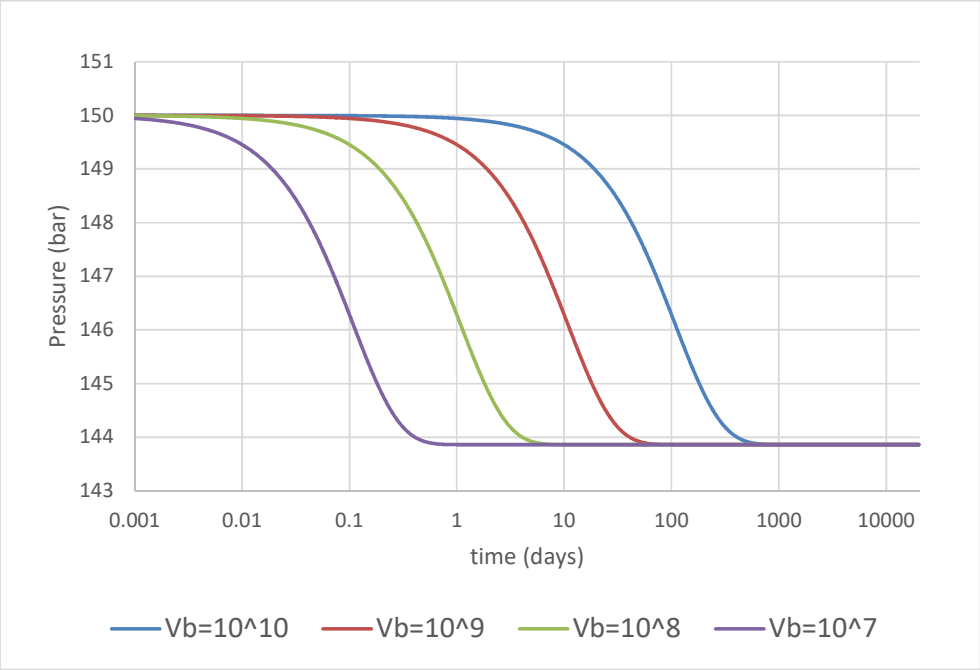

Figure 3.8 : Comparison of pressure behavior for various bulk volumes under constant flow rate production scenario.

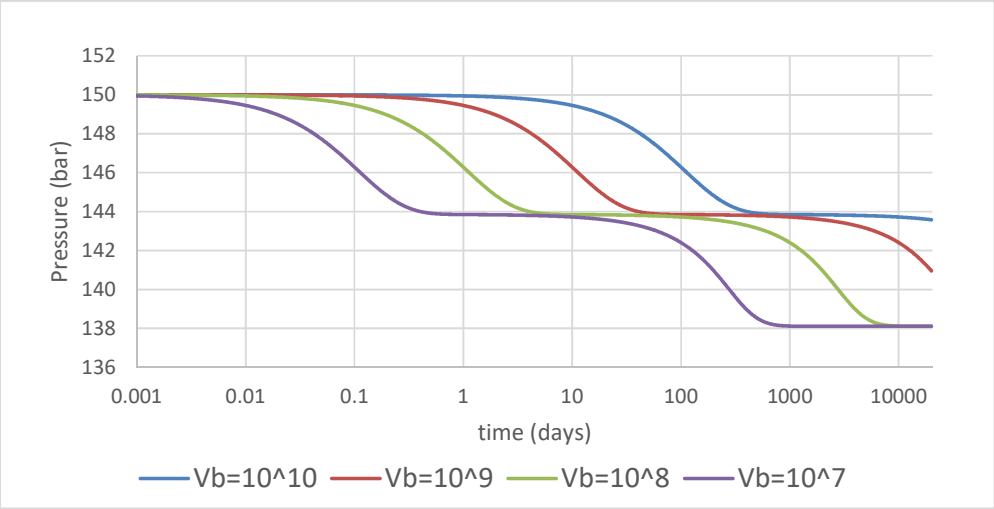

Figure 3.9 : Comparison of pressure behavior for various bulk volumes under constant energy production scenario.

Recall the steady state pressure drop solution derived in Chapter 2. Equation 2.19 indicates that at late time, the reservoir pressure drop stabilizes at an equilibrium value determined by the net production rate. The pressure decline becomes independent of the reservoir storage coefficient, κ and bulk volume, V_b.

For constant flow rate production scenario, which is w_p=307 kg/s (which is the required production rate for 50 MW_e considering initial conditions), steady state pressure drop for all bulk volumes will be;

$$\Delta p_{ss} \cong 0.02 w_p = 0.02 x 307 \cong 6.14 \text{ bar}$$

$$p_{ss} \cong p_0 - \Delta p_{ss} \cong 150 - 6.14 \cong 143.86 \text{ bar}$$

For constant energy production scenario, using equation 2.26, steady state pressure will be calculated as:

$$\Delta p_{ss} \cong \frac{(1-x)e_p}{C_{wp} T_{ss} \eta \alpha} \cong \frac{(1-0.8) x 50 x 10^6}{4273 x 131.2 x 0.15 x 10} \cong 11.89 \text{ bar}$$

$$p_{ss} \cong p_0 - \Delta p_{ss} \cong 150 - 11.89 \cong 138.11 \text{ bar}$$

Twice pressure stabilizations observed in Fig. 3.9 can be explained by the same reason discussed in the base case.

Second Case

In the second case, $V_b = 10^8$ m^3, $\phi = 0.05$, $w_i = 0.8 x w_p$, $\alpha = 10$ kg/bar-s. This case discusses the effects of various e_p (installed power capacity) values on the reservoir pressure and temperature under both scenarios. All the other reservoir parameters will be kept same as in the base case except the e_p value.

The V_b, ϕ, w_i, α and other reservoir parameters are fed into the model to regenerate the pressure and temperature behavior over 20000 days. Model has been run five times for various e_p values of $e_p = 10$ MW$_e$, $e_p = 20$ MW$_e$, m^3, $e_p = 50$ MW$_e$, $e_p = 80$ MW$_e$ and e_p=100 MW$_e$.

The temperature and pressure profiles of the reservoir for various e_p values over 20000 days under constant flow rate production and constant energy production scenarios are shown in figures below. Graphs indicate that geothermal reservoir at the end of 20000 days has reached to its steady state boundaries when e_p=100 MW$_e$, e_p=80 MW$_e$, e_p=50 MW$_e$. Fig. 3.10 and Fig. 3.11 show that temperatures at late time stabilize at the same value under both scenarios. As it is clarified in the base case, steady state temperature depends on C_{wp} only, regardless of the scenario. Since C_{wp} stabilizes at 4273 J/kg-^{0}C, steady state temperature is 131.2 ^{0}C.

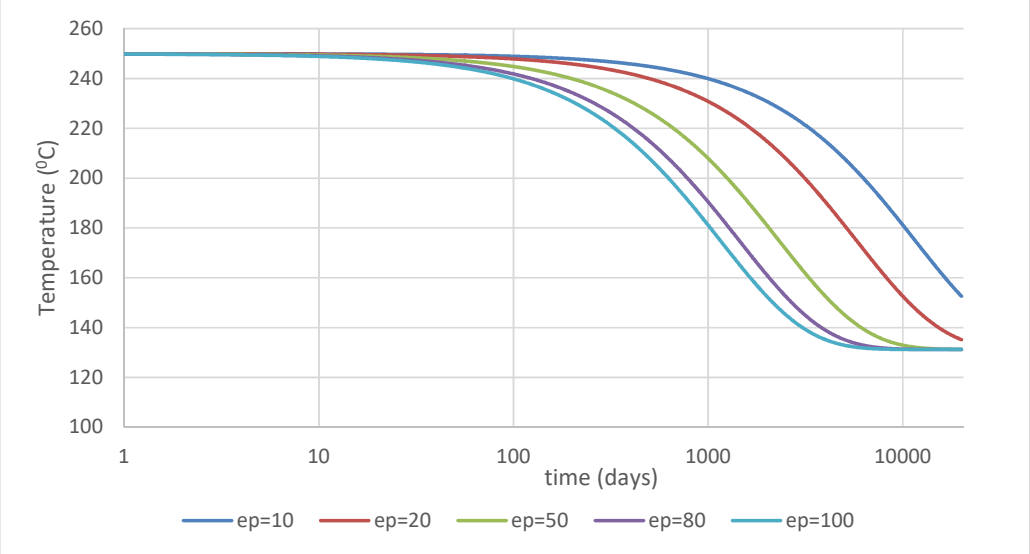

Figure 3.10 : Comparison of temperature behavior for various e_p values under constant flow rate production scenario.

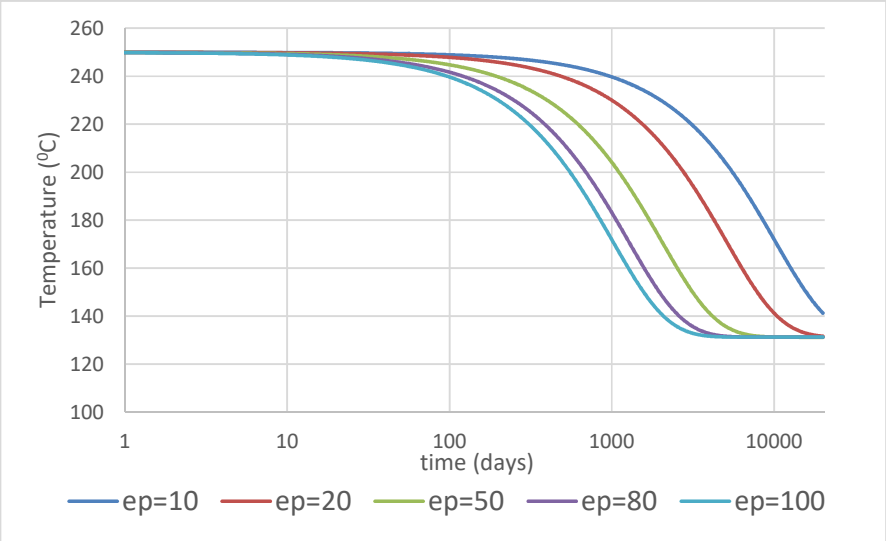

Figure 3.11 : Comparison of temperature behavior for various e_p values under constant energy production scenario.

When analyzing Fig. 3.12, it is seen that the steady state production rates for various e_p values are different. It is explained by equation 2.23;

$$w_{p\_ss} = \frac{e_p}{C_{wp} T_{ss} \eta} = \frac{e_p}{4273x131.2x0.15} = 1.189x10^{-5} e_p \tag{3.3}$$

Equation 3.3 shows that production flow rate at late time depends on the e_p value.

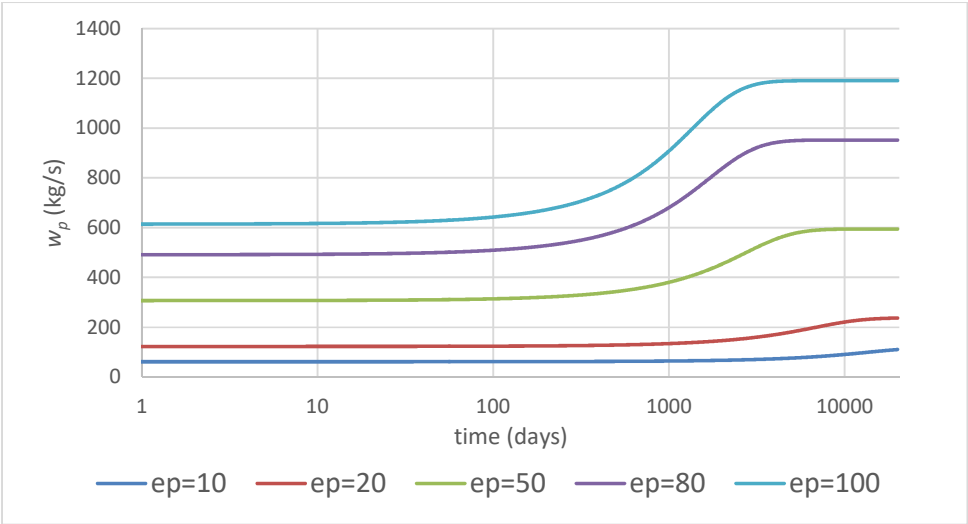

Figure 3.12 : Change of flow rate productions with time for various e_p values under constant energy production scenario.

Fig. 3.13 and Fig. 3.14 indicate that reservoir pressure has stabilized at various values for e_p=100 MW_e, e_p=80 MW_e, e_p=50 MW_e. Let's recall the pressure solution for constant energy production at late time to understand this case. From equation 2.26;

$$\Delta p_{ss} \cong \frac{(1-0.8)e_p}{4273x131.2x0.15x10} \cong 2.38x10^{-7} e_p \tag{3.2}$$

Equation 3.2 shows that steady state pressure under constant energy production scenario depends on the e_p value. Hence, for each e_p value, steady state pressure value will be different.

For e_p =100 MW_e, Δp_{ss}=2.38x10^{-7}x100x10^6=23.8 bar,

p_{ss}≅150-23.8≅126.2 bar

For e_p =80 MW_e, Δp_{ss}=2.38x10^{-7}x80x10^6=19.04 bar,

p_{ss}≅150-19.04≅130.96 bar

For e_p =50 MW_e, Δp_{ss}=2.38x10^{-7}x50x10^6=11.9 bar,

p_{ss}≅150-11.9≅138.1 bar

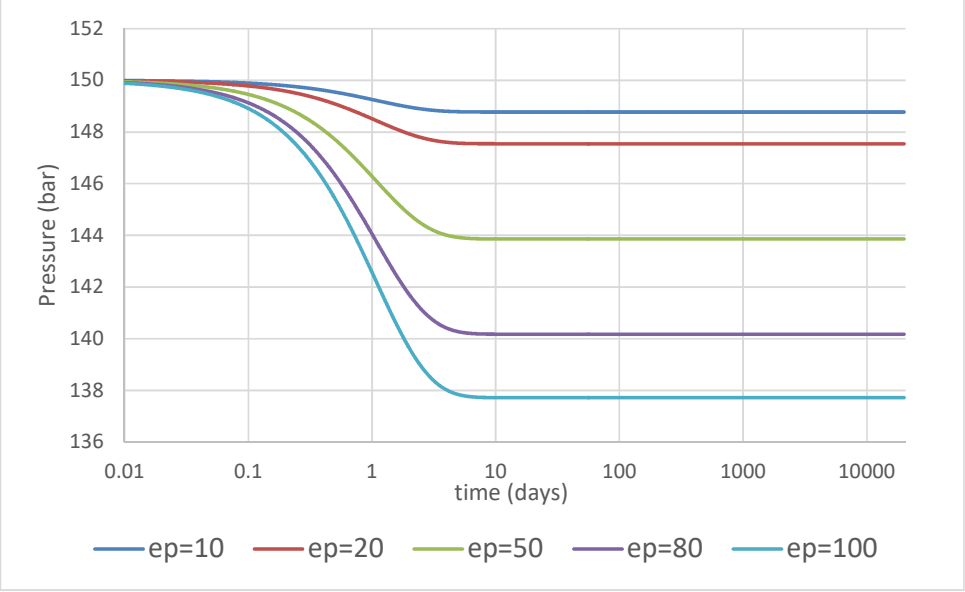

Figure 3.13 : Comparison of pressure behavior for various e_p values under constant flow rate production scenario.

For constant flow rate production, we determine production rate, w_p from equation 2.23 and w_i from equation 2.25;

$$w_p = \frac{e_p}{C_{wp} T \eta} = \frac{e_p}{4344.6x250x0.15} = 6.13x10^{-6} e_p$$

For e_p =100 MW_e, w_p=614 kg/s , w_i=491 kg/s ,

For e_p =80 MW_e, w_p=491 kg/s, w_i=393 kg/s ,

For e_p =50 MW_e, w_p=307 kg/s, w_i=245 kg/s ,

From equations 2.20 and 2.12, we get steady state pressure values as;

For e_p =100 MW_e, p_{ss} =137.72 bar

For e_p =80 MW_e, p_{ss} =140.18 bar

For e_p =50 MW_e, p_{ss} =143.86 bar

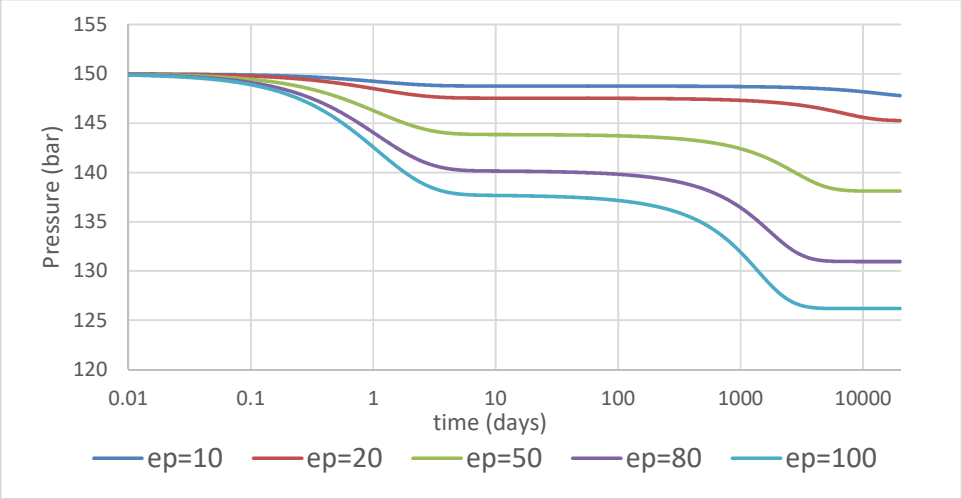

Figure 3.14 : Comparison of pressure behavior for various e_p values under constant energy production scenario.

Third Case

In the third case, $V_b = 10^8$ m^3, $e_p = 50$ MW_e, $w_i = 0.8x w_p$, $\alpha = 10$ kg/bar-s. The changing parameter is ϕ. This case discusses the effects of various porosity values on the reservoir pressure and temperature under both scenarios. All the other reservoir parameters will be kept same as in the base case except the porosity value, ϕ.

The V_b, e_p, w_i , α and other reservoir parameters are given into the model to generate the pressure and temperature behavior over 20000 days. Model has been run four times for various porosity values of ϕ= 0.01, ϕ= 0.05, ϕ= 0.1 and ϕ= 0.2. The pressure and temperature profile of the reservoir for various porosity values over 20000 days under both scenarios are shown in the figures below.

Fig. 3.15 to Fig. 3.19 show that for both constant energy production and constant flow rate production scenarios, reservoir reaches steady state flow regime in all porosity values. We know from previous cases that, in late time, for both scenarios neither temperature nor pressure depend on the porosity values. Equations 2.19 and 2.39 explain the temperature and pressure profiles at late time. Porosity shows its effect on very early days. When analyzing Fig. 3.17, it is also observed that under constant energy production scheme, porosity does not have any effect on flow rate production at late time.

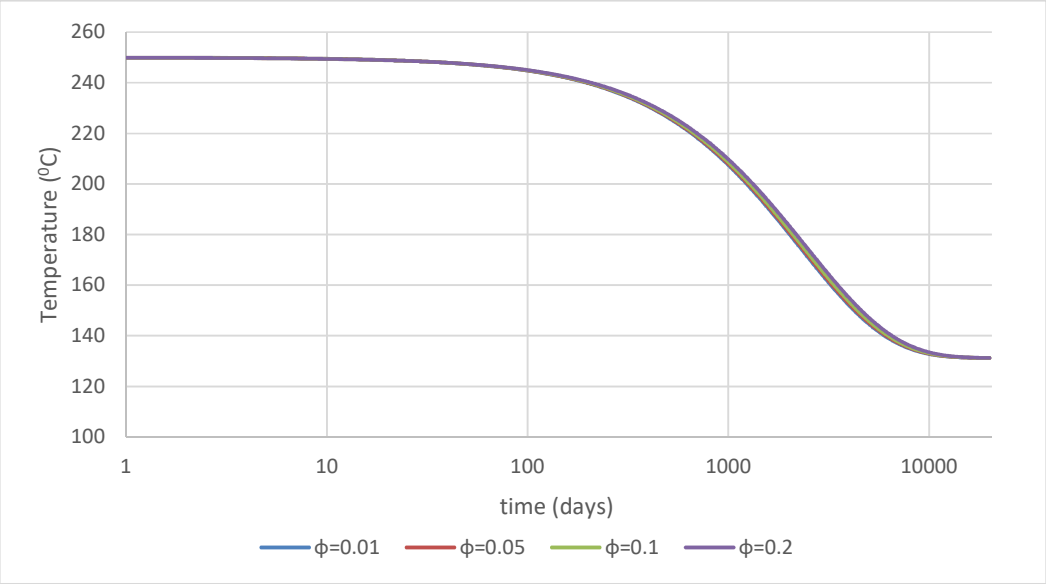

Figure 3.15 : Comparison of temperature behavior for various porosity values under constant flow rate production scenario.

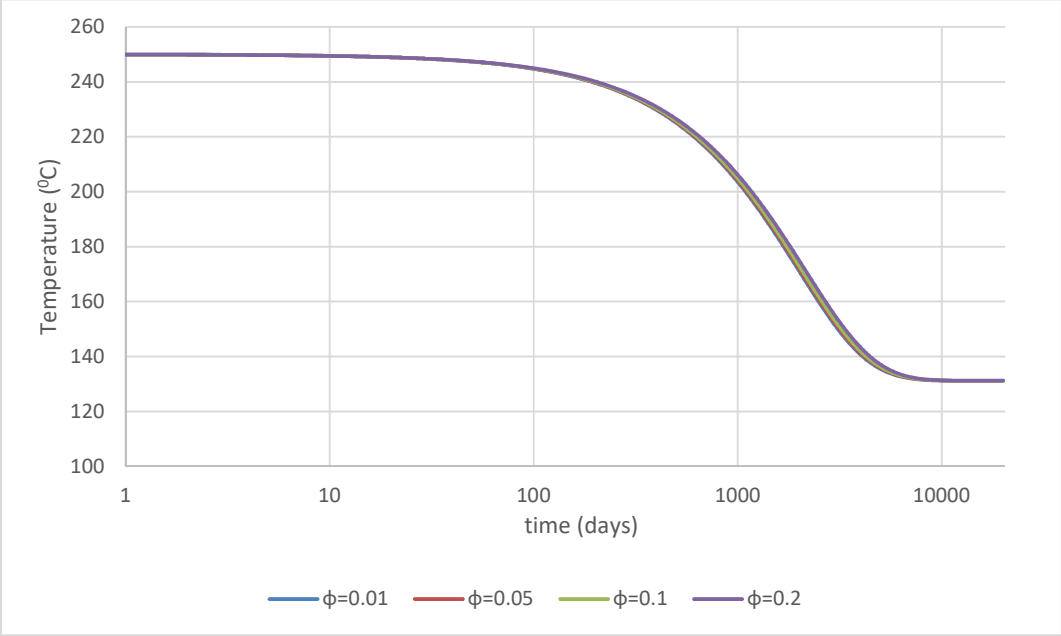

Figure 3.16 : Comparison of temperature behavior for various porosity values under constant energy production scenario.

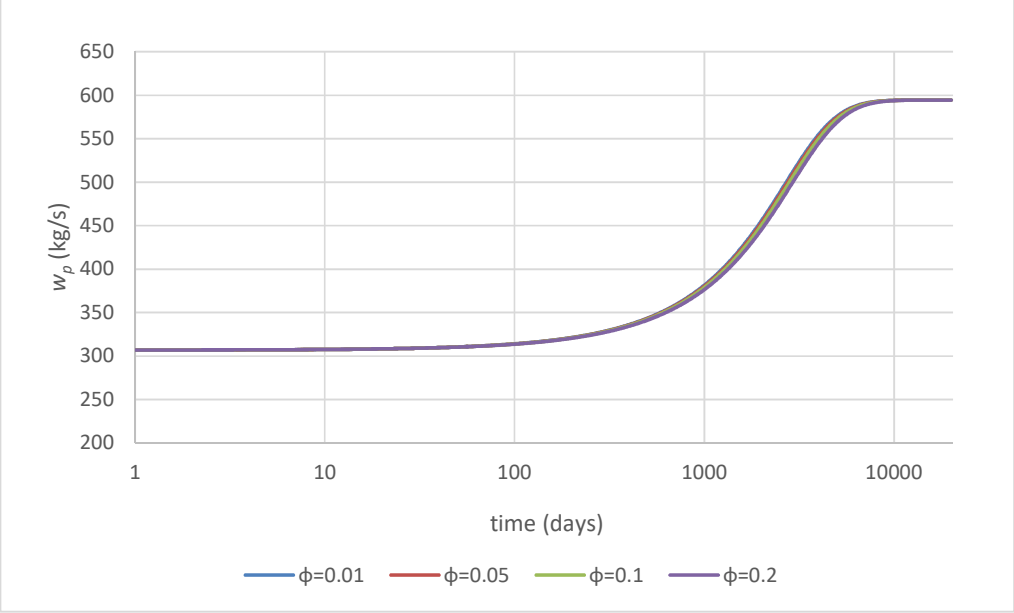

Figure 3.17 : Change of flow rate productions with time for various porosity values under constant energy production scenario.

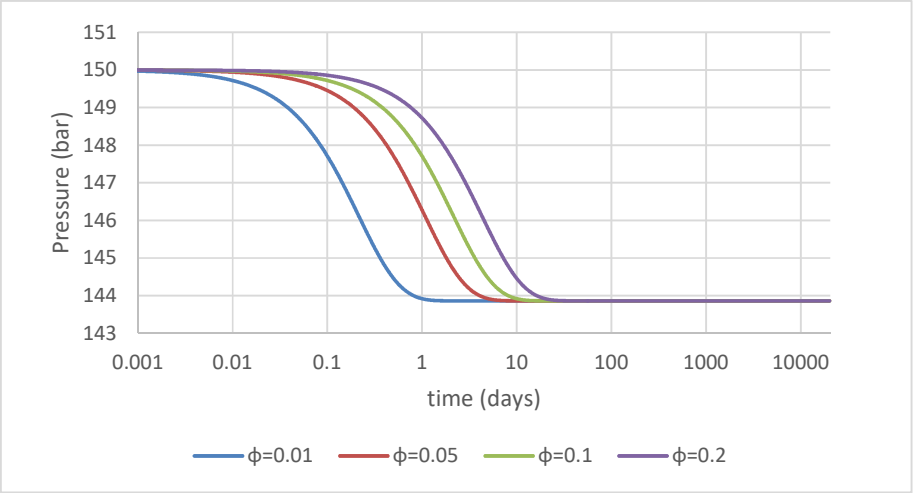

Figure 3.18 : Comparison of pressure behavior for various porosity values under constant flow rate production scenario.

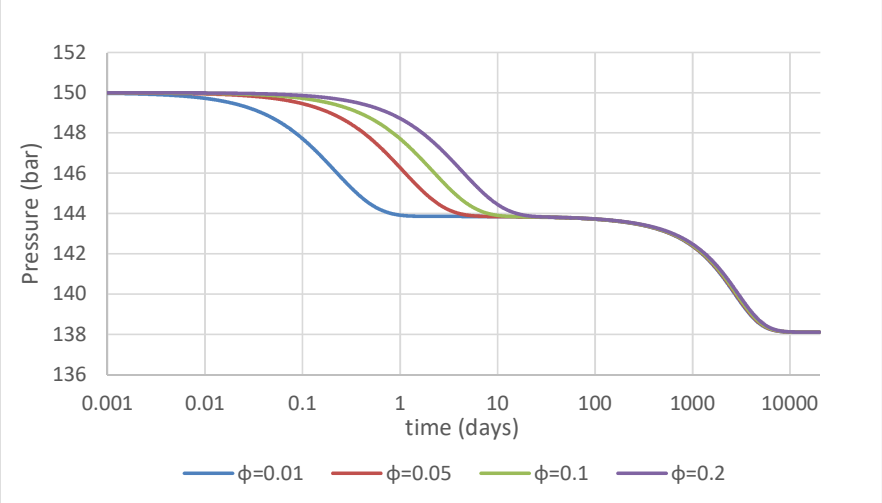

Figure 3.19 : Comparison of pressure behavior for various porosity values under constant energy production scenario.

Fourth Case

In the fourth case, $V_b = 10^8$ m^3, $e_p = 50$ MW$_e$, $\phi = 0.05$, $\alpha = 10$ kg/bar-s. The changing parameter is the reinjection ratio, x. The effects of the reinjection ratio on the reservoir pressure and temperature will be discussed under both scenarios in this case.

The V_b, e_p, ϕ, α and other reservoir parameters are fed into the model to regenerate the pressure and temperature profiles over 20000 days. Model has been run five times for various reinjection ratios, $x = 0, x$=0.5, x=0.8, x=0.9, and x=1, where the injection rates

will be $w_i = 0, w_i = 0.5w_p, w_i = 0.8w_p, w_i = 0.9w_p$, and $w_i = w_p$. The pressure and temperature profile of the reservoir under both scenarios are shown in the figures below.

Fig. 3.20 and Fig. 3.21 show that steady state temperatures for each injection rate, w_i are different. To explain Fig. 3.19 and Fig. 3.20, let's consider the temperature solution at late time. Recall equation 2.39, which indicates that steady state temperature does not depend on the production rate, w_p and injection rate, w_i, but depends on the reinjection ratio, x and specific heat capacity of the produced water, C_{wp}. This explains why temperature for both scenarios stabilizes at different values with various reinjection ratios.

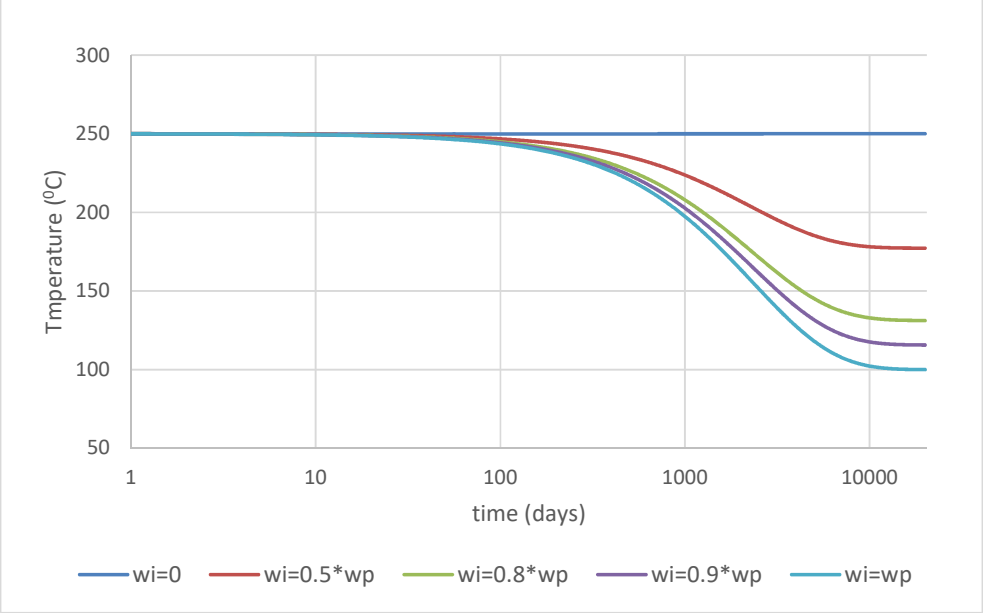

Figure 3.20 : Comparison of temperature behavior for various reinjection ratios under constant flow rate production scenario.

When analyzing Fig. 3.22, we see that for each injection rate, flow rate production at late time is different. This case again can be explained by equation 2.23;

$$w_{p\_ss} = \frac{e_p}{C_{wp}T_{ss}\eta} = \frac{50x10^6}{C_{wp}T_{ss}x0.15} = \frac{333.3x10^6}{C_{wp}T_{ss}}$$

Since for each injection rate, steady state temperature and specific heat capacity of the produced water is different, steady state production rate will also be different.

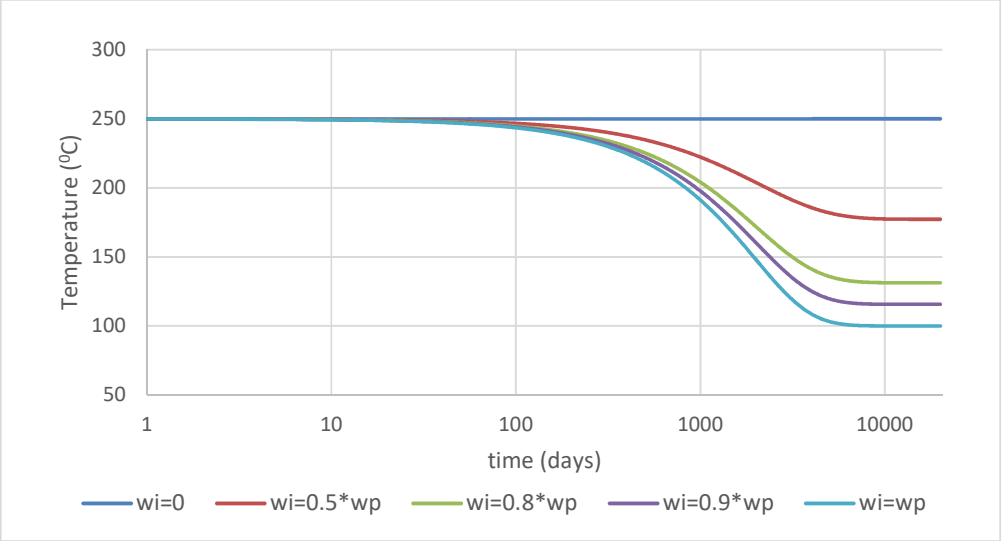

Figure 3.21 : Comparison of temperature behavior for various reinjection ratios under constant energy production scenario.

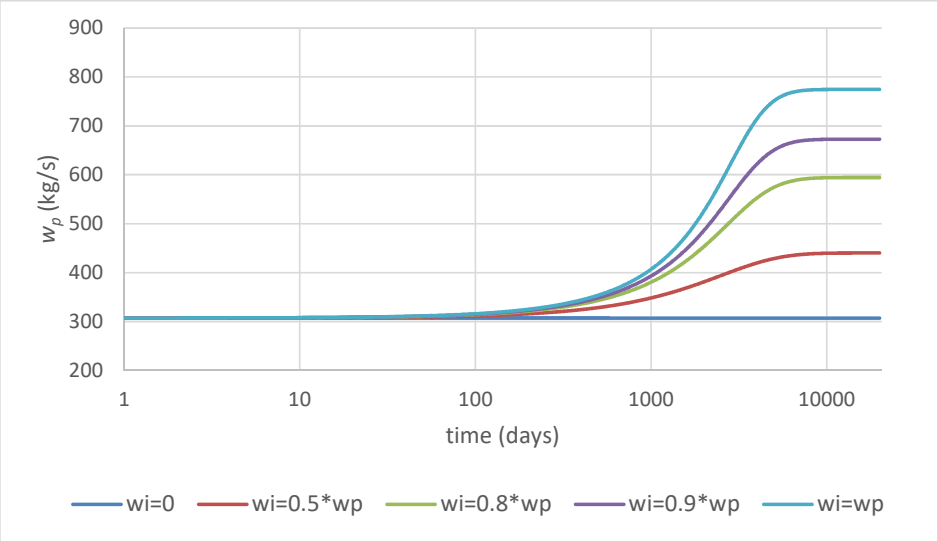

Figure 3.22 : Change of flow rate production with time for various injection rates under constant energy production scenario.

Fig. 3.23 and Fig. 3.24 show that steady state pressures are different for each injection rate and each scenario.

Now we will consider steady state pressure solution for constant flow rate production scenario. Recall equation 2.26, which indicates that late time pressure at constant flow

rate production depends on the production rate, w_p and the reinjection ratio, x when α is constant. Equation 2.26 explains why steady state pressure is getting higher as reinjection ratio, x getting larger.

Now we will consider the late time pressure drop solution for constant energy production. Recall equation 2.26,

$$\Delta p_{ss} \cong \frac{w_{net}}{\alpha} \cong \frac{w_p - w_i}{\alpha} \cong \frac{(1-x)w_p}{\alpha} \cong \frac{(1-x)e_p}{C_{wp}T_{ss}\eta\alpha}$$

which shows that at late time pressure drop depends on temperature, T, specific heat capacity C_{wp} and the reinjection ratio, x. That is why steady state pressures are different for various values of injection rates.

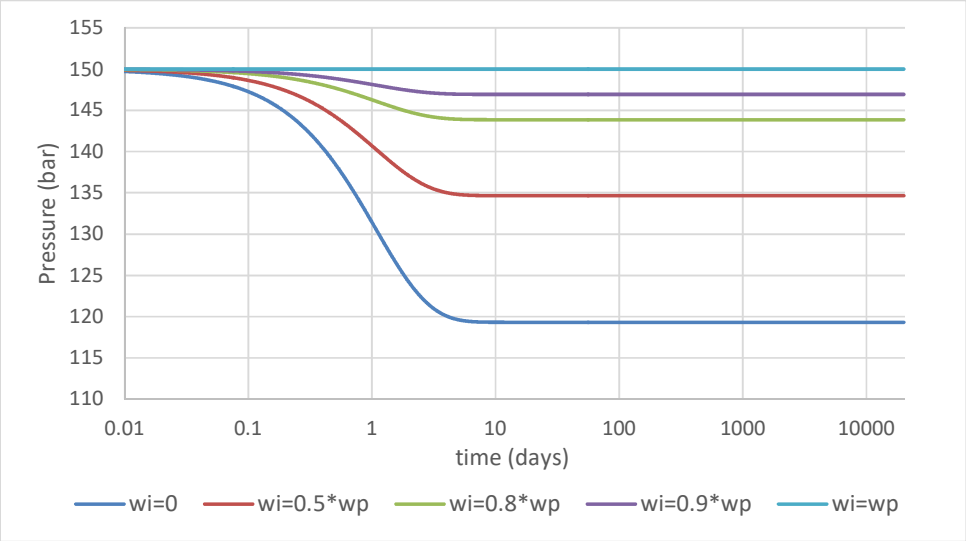

Figure 3.23 : Comparison of pressure behavior for various reinjection ratios under constant flow rate production scenario.

Twice pressure stabilizations under constant energy production for various injection rates can be explained by the same reason discussed in the base case. The interesting point in this case is that pressure curve for w_i=0 is different than the pressure curves of other injections rates. It has only one stabilization pressure which is actually the steady state pressure. To understant this pressure behavior we need to look at the temperature behavior of the same case. Fig. 3.21 shows that temperature has not decreased from the beginning. From equation 2.37 we know that temperature is

determined by the injection temperature and recharge temperature. Since injection rate is zero, reservoir temperature will be determined only by the recharge temperature Because recharge source temperature is equal to initial reservoir temperature in our study, temperature will not decrease with time. Since temperature does not change, flow rate production will be constant under constant energy production scenario. That means pressure profile will be same as in the constant flow rate production scenario.

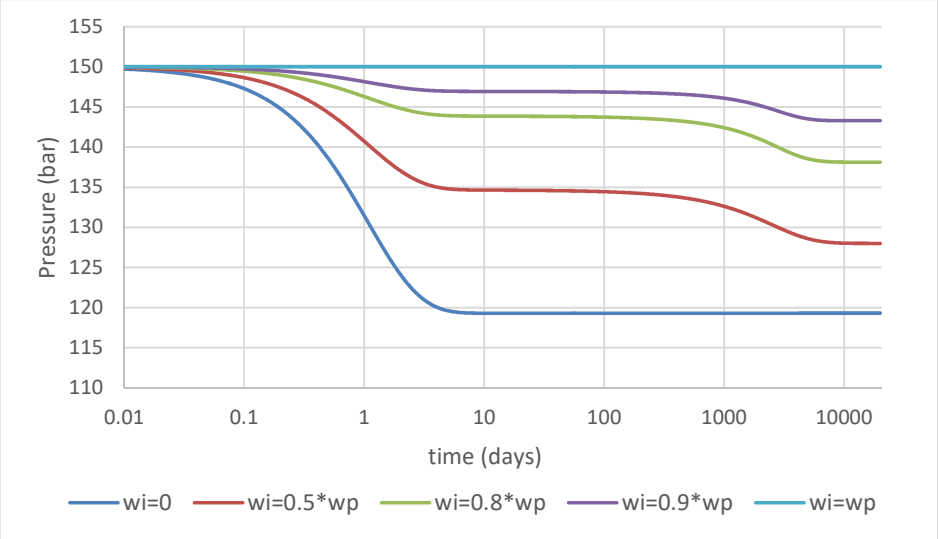

Figure 3.24 : Comparison of pressure behavior for various injection rates under constant energy production scenario.

Fifth Case

In this case $V_b = 10^8$ m^3, $e_p = 50$ MW$_e$, $\phi = 0.05$, $w_i = 0.8 x w_p$. The changing parameter is the recharge constant, α. This case will discuss the effects of recharge constant on reservoir performance behavior over 20000 days. Model has been run four times for each value of recharge constant, α=5 kg/bar-s, α=10 kg/bar-s, α=30 kg/bar-s and α=50 kg/bar-s and pressure and temperature profile has been generated.

Fig. 3.25 and Fig. 3.26 show that temperature at late time is the same value for each α value and for each scenario. As equation 2.39 declares, temperature at late time does not depend on the recharge constant. That explains why temperature at late time for each recharge constant and for each scenario is the same value.

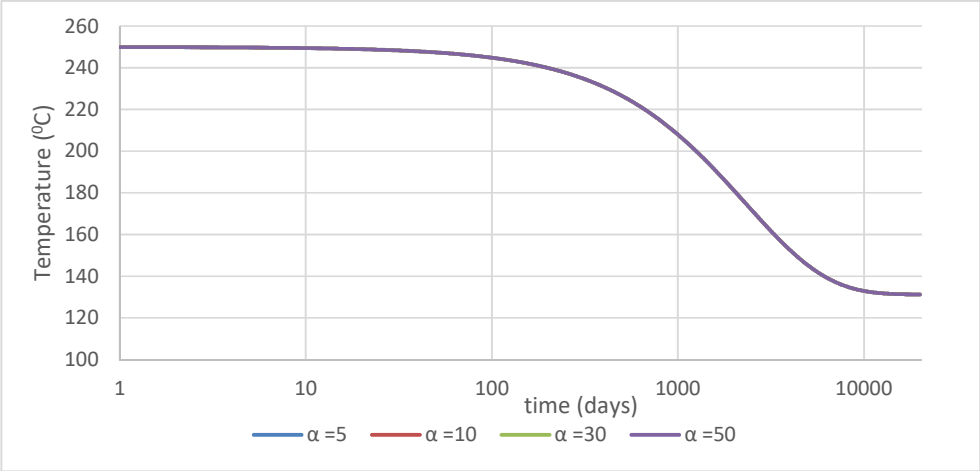

Figure 3.25 : Comparison of temperature behavior for various α values under constant flow rate production scenario.

Fig. 3.27 shows that flow rate production does not change with the recharge constant value. Since temperature and specific heat capacity at late time is the same for each α value, flow rate at late time for each case will be same, too. In other words, flow rate production at late time is independent of recharge constant.

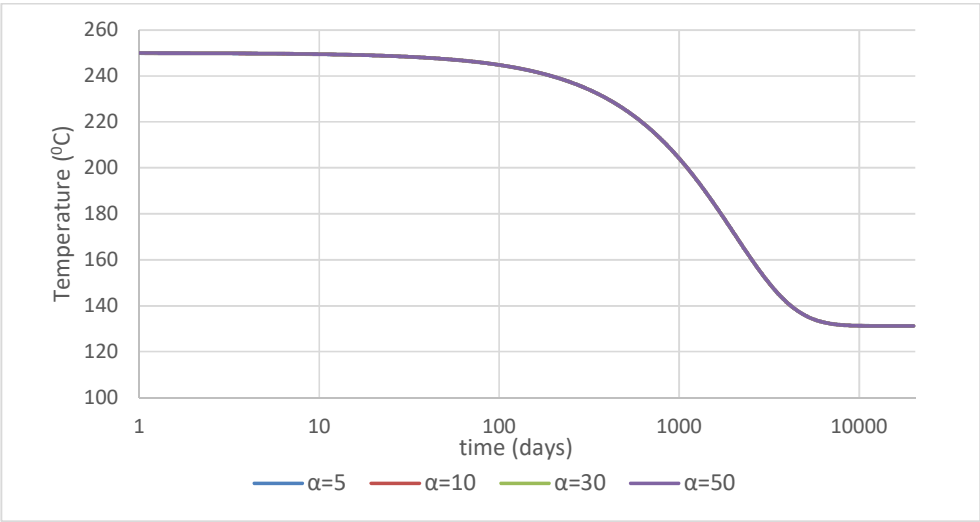

Figure 3.26 : Comparison of temperature behavior for various α values under constant energy production scenario.

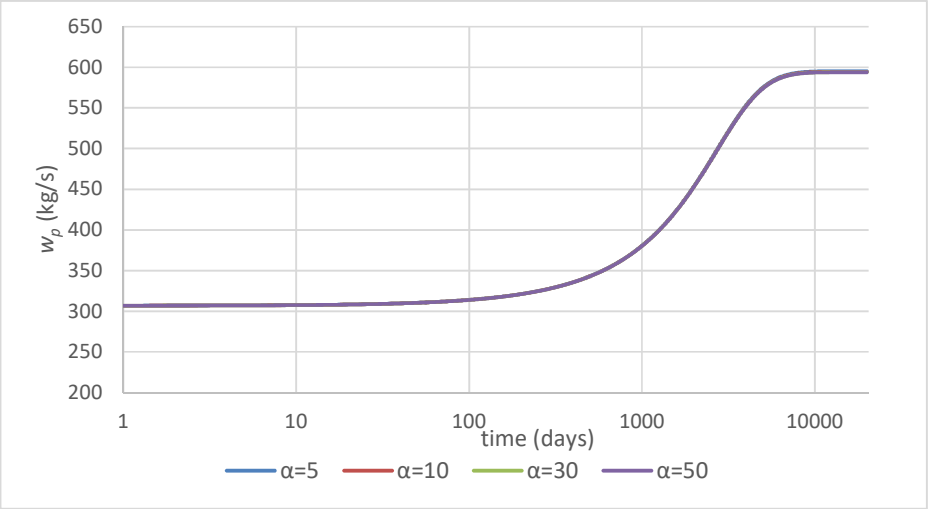

Figure 3.27 : Change of flow rate production with time for various α values under constant energy production scenario.

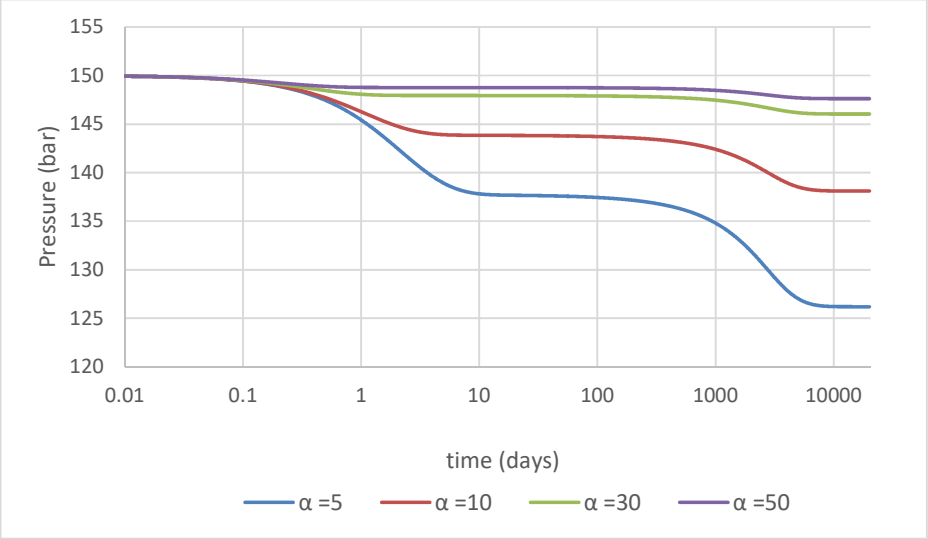

Figure 3.28 : Comparison of pressure behavior for various α values under constant energy production scenario.

When analyzing Fig. 3.28 and Fig. 3.29 we see that stabilization pressure is different for each scenario and for each α value. As discussed before, equation 2.19 shows that steady state pressure drop is dependent on recharge constant and net production rate. Since net production rate and recharge constant are different in each scenario, stabilization pressure will be different under both scenarios for various α values.

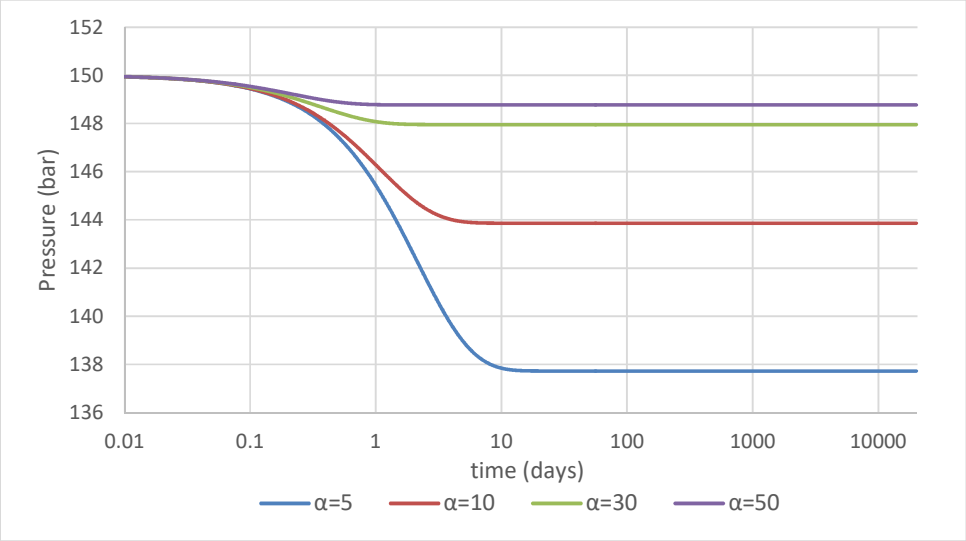

Figure 3.29 : Comparison of pressure behavior for various α values under constant flow rate production scenario.

4. CONCLUSIONS

Several lumped parameter models have been proposed in the literature previusly, some of which have been successfully used to simulate data from well known geothermal fields. However most of them are valid for isothermal geothermal fields and/or constant flow rate production scheme. In this study, a new non-isothermal single tank model has been developed to be used for both constant flow rate production and constant energy production scenarios. This study compares pressure and temperature profiles under both scenarios and discusses the effects of several parameters on reservoir performance behavior under constant energy production scheme. The following conclusions are obtained from this study;

- When considering pressure and temperature profiles, it is observed that pressure and temperature at late time for constant energy production scenario stabilizes at some value like in the constant flow rate production scenario.
- When considering flow rate production change for constant energy production scenario, it is concluded that flow rate production is dependent on temperature and specific heat capacity of the produced water. Since at late time temperature and specific heat capacity of the water stabilizes at some value, flow rate production also stabilizes at late time.
- It is observed that bulk volume has effect on the pressure and temperature of the reservoir at early time and middle time. However, steady state pressure is the same for all bulk volumes.
- While installed power capacity is observed to affect the reservoir steady state pressure, it has no effect on the steady state temperature for constant energy production scheme.
- It is observed that steady state pressure and temperature are not affected by the rock porosity under both scenarios.
- Since pressure and temperature at late time depend on the injection rate, they will stabilize at different values for various values of reinjection ratio.
- While recharge constant has no effect on the steady state temperature, it affects steady state pressure under constant energy production scheme.

REFERENCES

Alkan, H. and Satman, A. (1990): A New Lumped-parameter Model for Geothermal Reservoirs in the Presence of Carbon Dioxide. Geothermics 19, 469-479.

Antics, M., Bertani, R. and Sanner, B. (2016): Summary of EGC 2016 Country Update Reports on Geothermal Energy in Europe. European Geothermal Congress 2016, Strasbourg, France, 19-24 Sept.

Axelsson, G. (1989): Simulation of Pressure Response Data from Geothermal Reservoirs by Lumped-parameter Models. Proceedings of the 14th Workshop on Geothermal Reservoir Engineering, Stanford University, Stanford, CA, USA, pp. 257-263.

Brigham, W.E. and Morrow, W.B. (1974): P/Z behavior for geothermal steam reservoirs. Paper SPE 4899 presented at the 44th Annual California Regional Meeting of the Society of Petroleum Engineers, AIME, San Francisco, California.

Brigham, W. E. and Neri, G. (1980): A Depletion Model for the Gabbro Zone (Northern Part of Larderello Field). Proceeding of the Second DOE-ENEL Workshop for Cooperative Research in Geothermal Energy, October 20-22, Lawrence Berkeley Laboratory Report LBL-11555, pp.434-463.

Castanier, L.M. and Brigham, W. E. (1983): Use of Lumped Parameter Modeling for Geothermal Engineering. Proceedings of SPE California Regional Meeting, SPE 11730, Ventura, CA, USA, March 23-25, pp.593-601.

Castanier, L.M., Sanyal, S. K. and Brigham, W. E. (1980): A Practical Analytical Model for Geothermal Reservoir Simulation. Proceedings of the 50th Annual California Regional Meeting of SPE, SPE 8887, Los Angeles, CA, USA, April 9-11.

Grant, M. A., Donaldson, I. G. and Bixley, P. F. (1982): Geothermal Reservoir Engineering. Academic Press, New York, pp. 369.

Holm, A., Jennejohn, D. and Blodgett, L. (2012): Geothermal Energy and Greenhouse Gas Emissions. Geothermal Energy Association, November.

Lund, J. W., Boyd, T.L. (2015): Direct Utilization of Geothermal Energy 2015 Worldwide Review, Proceedings World Geothermal Congress 2015, Melbourne, Australia, 19-25 April.

Matek, B. (2016): Annual U.S. & Global Geothermal Power Production Report, Geothermal Energy Association, March.

Onur, M., Sarak, H., Türeyen, O. I., Cinar, M., and Satman, A. (2008): A New Non-Isothermal Lumped-Parameter Model for Low Temperature, Liquid Dominated Geothermal Reservoirs and Its Applications. Proceedings of the 33rd Workshop on Geothermal Reservoir Engineering, Stanford University, Stanford, California, January 28-30.

Sarak, H. (2004): Lumped Parameter Models for Low-Temperature Geothermal Reservoirs, Ph.D. Thesis, Istanbul Technical University, April.

Sarak, H., Onur, M., and Satman, A. (2005): Lumped Parameter Models for Low Temperature Geothermal Fields and Their Application. Geothermics 34 (2005) 728-755, October 10.

Türeyen, O. I., Akyapi, E. (2010): A Generalized Non-Isothermal Tank Model for Liquid Dominated Geothermal Reservoirs. Geothermics 40 (2011) 50–57.

Türeyen, O. I., Onur, M., and Sarak, H. (2007): Assessing Uncertainity in Future Pressure Changes Predicted by Lumped-parameters. A Field Applications, 32nd Workshop on Geothermal Reservoir Engineering, Stanford University, Stanford, California, January 22-24.

Türeyen, O. I., Onur, M., and Sarak, H. (2009): A generalized non-isothermal lumped-parameter model for liquid dominated geothermal reservoirs. Proceedings of the 34th Workshop on Geothermal Reservoir Engineering, Stanford University, Stanford, California, February 9-11

Url-1 <https://www.geothermal-energy.org)>, date retrieved 14.07. 2016

Westwood, J. D., Castanier, L. M. (1981): App1ication of a Lumped Parameter Model to the Cerro Prieto Geothermal Field. Proceedings of the Seventh Workshop Geothermal Reservoir Engineering Stanford, December 15-17.

Whiting, R.L. and Ramey Jr., H. J. (1969): Application of Material and Energy Balances to Geothermal Steam Production. Journal of Petroleum Technology 21, 893-900.

CURRICULUM VITAE

Name Surname **: Gunay TAHIROVA**

Place and Date of Birth **: Azerbaijan, 01.01.1987**

E-mail **: gny.thr@gmail.com**

EDUCATION

- **B.Sc.** **:** 2009, Middle East Technical University, Petroleum and Natural Gas Engineering Department

PROFESSIONAL EXPERIENCE AND REWARDS:

- 2009-2010 Project Engineer in the department of "Development of oil and gas deposits" at State Oil Company of Azerbaijan Republic, Baku
- 2010-2012 LMWD Field Engineer in Schlumberger, Baku